7
Carbohydrates

Gerald Dräger, Andreas Krause, Lena Möller, and Severian Dumitriu

7.1
Introduction

Polysaccharides are an integral part of the living matter. Due to this huge presence in organisms, they are highly biocompatible and biodegradable and therefore idealy match the basic characteristics for polymers used as biomaterials.

All polysaccharides used derive from natural sources. Biodegradation is defined as an event which takes place in the natural environment and living organisms. Since polysaccharides are ubiquitous in nature and present a valuable carbon and energy source in the life cycle of organisms, their biodegradation is a highly evolved process using effective and usually specific enzymes. This makes polysaccharides a promiscuous basis for the development of biodegradable polymers.

Polysaccharide-based biomaterials are of great interest in several biomedical fields such as drug delivery, tissue engineering, or wound healing. Important properties of the polysaccharides include controllable biological activity, biodegradability, and their ability to form hydrogels. Polysaccharides are also used as additives in the food industry and in many technical applications. Here the main focus lies on the superb rheological properties of many polysaccharides together with their biodegradability and their positive environmental and toxicological effects.

Several important and up-to-date reviews have to be mentioned and should be considered in order to gain insight in this complex topic. In 2008, Rinaudo summarized the main properties and current applications of some polysaccharides as biomaterials [1]. The application of biodegradable systems in tissue engineering and regenerative medicine with a strong focus on carbohydrates is summarized by Reis and coworkers [2]. Polysaccharides-based nanoparticles as drug-delivery systems are reviewed by Liu *et al.* [3], whereas Coviello *et al.* focused on polysaccharide hydrogels for modified release formulations [4]. In this chapter, we summarize the basic properties, modifications, and applications of biodegradable polysaccharides. We deliberately omit starch and pectin since there are numerous reviews and books dealing solely with these materials.

Handbook of Biodegradable Polymers: Synthesis, Characterization and Applications, First Edition. Edited by Andreas Lendlein, Adam Sisson.

7.2 Alginate

Alginate belongs to the family of linear (unbranched), nonrepeating copolymers. It consists of variable amounts of β-D-mannuronic acid (M) and its C5-epimer α-L-guluronic acid (G) which are linked via β-(1,4)-glycosidic bonds. The glycosidic bonds of mannuronic acid are connected to the following unit by a diequatorial $^4C_1$ linkage, while guluronic acids are diaxial $^1C_4$ linked. Alginate can be regarded as a true block copolymer composed of homopolymeric M and G regions, called M- and G-blocks, respectively, interspersed with regions of alternating structure [5] (Scheme 7.1).

The physicochemical properties of alginate have been found to be highly affected by the M/G ratio as well as by the structure of the alternating zones. In terms of specific medical applications, alginate materials with a high guluronic acid ratio exhibit a much better compatibility [6]. The first protocol to hydrolyze the glycosidic bonds of alginate has been published by Haug *et al*. in the 1960s and is based on a pH-dependent acid-catalyzed hydrolysis, which leads to a fragmentation of the polymeric chain. Breaking the glycosidic bonds of both building blocks selectively could be achieved due to different pK_a values of mannuronic acid (pK_a: 3.38) and guluronic acid (pK_a: 3.65) [7]. Therefore, polyguluronic acid can be separated by precipitation in aqueous conditions after protonating the carboxyl groups.

Alginate can be extracted from marine brown algae or it can be produced by bacteria. Both species produce alginate as an exopolymeric polysaccharide during their growth phase. Isolated alginates from marine brown algae like *Laminaria hyperborea* or *lessonia*, gained by harvesting brown seaweeds from coastal regions, tend to vary in their constitution due to seasonal and environmental changes. Like chitin in shellfish, alginates in algae have structure-forming functions. This is due to the intracellular formed gel matrix, which is responsible for mechanical strength, flexibility, and form. Alginates in bacteria are synthesized only by two genera, *Pseudomonas* and *Azotobacter*, and have been extensively studied over the last 40 years. While primarily synthesized in the form of polymannuronic acid, the biosynthesis undergoes chemical modifications comprising acetylation and epimerization, which occurs during periplasmic transfer and before final export through the outer membrane. Extracted alginate from *Pseudomonas* contains only M blocks

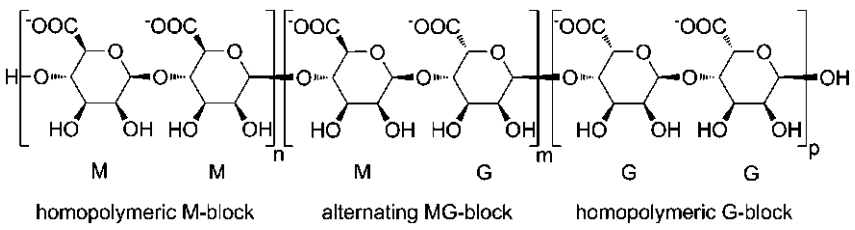

Scheme 7.1 Chemical structure of alginate with mannuronic acid (M), alternating, and guluronic acid (G) blocks.

and may be O-2 and/or O-3 acetylated. The G units are introduced by mannuronan C-5 epimerases. The genetic modification of alginate-producing microorganisms could enable biotechnological production of new alginates with unique, tailor-made properties, suitable for medical and industrial applications [5].

Depolymerization of alginate is catalyzed by different lyases. The depolymerization occurs by cutting the polymeric chain via β-elimination, generating a molecule containing 4-desoxy-L-erythro-hex-4-enepyranosyluronate at the nonreducing end. Such type of lyases have been found in organisms using alginate as a carbon source, in bacteriophages specific for alginate-producing organisms, and in alginate-producing bacteria [8]. In recent times, recombinant alginat lyases with different preferences for the glycosidic cleavage were published [9].

Alginate is a well-known polysaccharide widely used due to its gelling properties in aqueous solutions. The gelling is related to the interactions between the carboxylic acid moieties and bivalent counterions, such as calcium, lead, and copper. It is also possible to obtain an alginic acid gel by lowering the environmental pH value. Like DNA, alginate is a negatively charged polymer, imparting material properties ranging from viscous solutions to gel-like structures in the presence of divalent cations. Divalent ions at concentration of >0.1% (w/w) are sufficient for gel formation. The gelling process takes place by complexation of divalent cations between two alginate chains; primarily G building blocks interact with present cations. Since calcium ions interact with carboxyl functions of four G-units, the formed structure induces helical chains. This coordination geometry is generally known as "egg box" model [10, 11] (Scheme 7.2).

The fact that G-units are responsible for gelation leads to the attribute that alginate with a higher G content show higher moduli. Enriched high-G gels have more regular, stiff structures with short elastic segments. They obtain a more ridged, static network compared to the more dynamic and entangled structure of low-G gels with their long elastic segments [12]. Interactions with univalent cations in solution have been investigated by Seale *et al.* by circular dichroism and

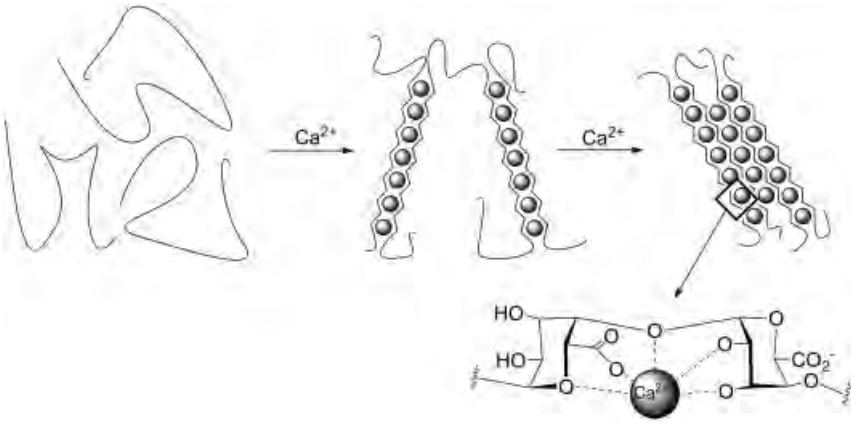

Scheme 7.2 Scheme of the egg box model; complexation of calcium via four G-units.

rheological measurements. Poly-L-guluronate chain segments show substantial enhancement (approximately 50%) of circular dichroism ellipticity in the presence of excess K^+, with smaller changes for other univalent cations: $Li^+ < Na^+ < K^+ > Rb^+ > Cs^+ > NH_4^+$ [13].

The only commercial available derivative of alginate is propylene glycol alginate, produced by esterification of the uronic acids with propylenoxide. Propylene glycol alginate is mostly utilized in food industry as stabilizer, thickener, and emulsifier. Other food additives are sodium alginate, ammonium alginate, calcium alginate (CA), and potassium alginate. All these alginate types with different cations are water soluble. In order to achieve solubility of alginate in polar organic solvents, it is necessary to exchange these cations by quaternary ammonium salts with lipophilic alkyl chains. Basically two strategies were pursued to modify the monomeric structure. On the one hand, the carboxyl group is attacked by a strong nucleophile, generally using an active ester as precursor. The second strategy uses a ring-opening of the carbohydrate by cracking the bonds between C-3 and C-4. Aqueous sodium periodate breaks vicinal diols generating two aldehydes [14]. A wide range of reactions in dimethyl sulfoxide or *N*,*N*-dimethylformamide are described, where different ester or amides could be synthesized [15]. Furthermore radical photo crosslinkable alginate has been synthesized by Jeon *et al*. via acrylating the carboxylic acid [16]. Several alginate derivatives have been synthesized to generate hydrogels. The generation of thermostable hydrogels can be achieved using UV radiation [17] or crosslink reagents [18, 19] for *in situ* polymerization. With regard to clinical applications, drugs or biomarker like methotrexate, doxorubicin hydrochloride, mitoxantrone dihydrochloride [20], daunomycin [21], or linear RGD-peptides [22] were attached to the alginate backbone. Afterward the modified alginates were gelled by adding calcium chloride or crosslink reagents, respectively.

Alginate with its unique material properties and characteristics has been increasingly considered as biomaterial for medical applications. Alginate has been used as excipient in tablets with modulated drug delivery. CA gels have unique intrinsic properties and exhibit biocompatibility, mucoadhesion, porosity, and ease of manipulation. Hence, much attention has recently been focused on the delivery of proteins, cell encapsulation, and tissue regeneration. Alginates play the role of an artificial extracellular matrix, especially in the area of tissue engineering, and alginate gels are widely used as wound regeneration materials [23–26].

Besides the commercially available wound dressing Kaltostat®, fibrous ropes composed of mixed calcium and sodium salts of alginic acid, new types of alginate-based dressings have been developed. Chiu *et al*. presented two new types by crosslinking alginate with ethylendiamine and polyethyleneimine, respectively. Due to the improved properties compared to Kaltostat®, the author predicts a great potential for clinical applications [25].

Diabetic foot ulcers (DFUs) are at risk of infection and impaired healing, placing patients at risk of lower extremity amputation. DFU care requires debridement and dressings. A prospective, multicentre study from Jude *et al*. compared clinical efficacy and safety of AQUACEL® hydrofiber dressings containing ionic silver (AQAg) with those of Algosteril CA dressings. When added to standard care with

appropriate off-loading, AQAg silver dressings were associated with favorable clinical outcomes compared with CA dressings, specifically in ulcer depth reduction and in infected ulcers requiring antibiotic treatment. This study reports the first significant clinical effects of a primary wound dressing containing silver on DFU healing [27].

In terms of drug/protein delivery, numerous applications of CA gel beads or microspheres have been proposed. As one example, alginate nanoparticles were prepared by the controlled cation-induced gelation method and administered orally to mice. A very high drug encapsulation efficiency was achieved in alginate nanoparticles, ranging from 70% to 90%. A single oral dose resulted in therapeutic drug concentrations in the plasma for 7–11 days and in the organs (lungs, liver, and spleen) for 15 days. In comparison to free drugs (which were cleared from plasma/organs within 12–24 h), there was a significant enhancement in the relative bioavailability of encapsulated drugs. As clinical application, alginate-based nanoparticulate delivery systems have been developed for frontline antituberculosis drug carriers (e.g., for rifampicin, isoniazid, pyrazinamide, and ethambutol) [28].

Another approach for the surface modification of CA gel beads and microspheres has been the chemical crosslinking of the shell around the alginate core. The approach based on the technique of coating CA gel microspheres has also been used to produce microcapsules. This technique is very promising for the macromolecular drug delivery in biomedical and biotechnological applications [29]. Mazumder *et al.* have shown that covalently crosslinked shells can be formed around CA capsules by coating with oppositely charged polyelectrolytes containing complementary amine and acetoacetate functions. Furthermore, alginate gels were used for cell and stem cell encapsulation [30]. An approach of Dang *et al.* enables a practical route to an inexpensive and convenient process for the generation of cell-laden microcapsules without requiring any special equipment [31].

CA has been one of the most extensively investigated biopolymers for binding heavy metals from dilute aqueous solutions in order to engineer medical applications. Becker *et al.* have studied the biocompatibility and stability of CA in aneurysms *in vivo*. They depicted that CA is an effective endovascular occlusion material that filled the aneurysm and provided an effective template for tissue growth across the aneurysm neck after 30 to 90 days. The complete filling of the aneurysm with CA ensures stability, biocompatibility, and optimal healing for up to 90 days in swine [32].

Hepatocyte transplantation within porous scaffolds has being explored as a treatment strategy for end-stage liver diseases and enzyme deficiencies. The limited viability of transplanted cells relies on the vascularization of the scaffold site which is either too slow or insufficient. The approach is to enhance the scaffold vascularization before cell transplantation via sustained delivery of vascular endothelial growth factor, and by examining the liver lobes as a platform for transplanting donor hepatocytes in close proximity to the host liver. The conclusion by Kedem *et al.* has shown that sustained local delivery of vascular endothelial growth factor-induced vascularization of porous scaffolds implanted on liver lobes and improved hepatocyte engraftment [33].

Furthermore, sodium alginate is used in gastroesophageal reflux treatment [34, 35]. Dettmar *et al.* published the rapid effect onset of sodium alginate on gastroesophageal reflux compared with ranitidine and omeprazole [36]. The rate of acid and pepsin diffusion through solutions of sodium alginate was measured using *in vitro* techniques by Tang *et al.* They demonstrated that an adhesive layer of alginate present within the esophagus limits the contact of refluxed acid and pepsin with the epithelial surface [37].

In the field of nerve regeneration, Hashimoto *et al.* have developed a nerve regeneration material consisting of alginate gel crosslinked with covalent bonds. One to two weeks after surgery, regenerating axons were surrounded by common Schwann cells, forming small bundles, with some axons at the periphery being partly in direct contact with alginate. At the distal stump, numerous Schwann cells had migrated into the alginate scaffold 8–14 days after surgery. Remarkable restorations of a 50-mm gap in cat sciatic nerve were obtained after a long term by using tubular or nontubular nerve regeneration material consisting mainly of alginate gel [38].

7.3 Carrageenan

Carrageenan is a class of partially sulfated linear polysaccharides produced as main cell wall material in various red seaweeds (Rhodophyceae). The polysaccharide chain is composed of a repeating unit based on the disaccharide →3)-β-D-galactose-(1→4)-α-3,6-anhydro-D-galactose or →3)-β-D-galactose-(1→4)-α-D-galactose. Three major types can be distinguished by the number and position of the sulfate groups on the disaccharide repeating unit: κ-carrageenan (one sulfate group at position 4 of the β-D-galactose), ι-carrageenan (one sulfate group at position 4 of the β-D-galactose and one sulfate group at position 2 of the α-3,6-anhydro-D-galactose), and λ-carrageenan (one sulfate group at position 2 of the β-D-galactose and two sulfate groups at position 2 and 6 of the α-D-galactose) [39] (Scheme 7.3).

Different seaweeds produce different types of carrageenan but the biosynthesis of these commercially important polysaccharides is not completely studied yet. The most important subtype κ-carrageenan is isolated from the tropical seaweed *Kappaphycus alvarezii*, also known as *Eucheuma cottonii*. After alkali treatment, a

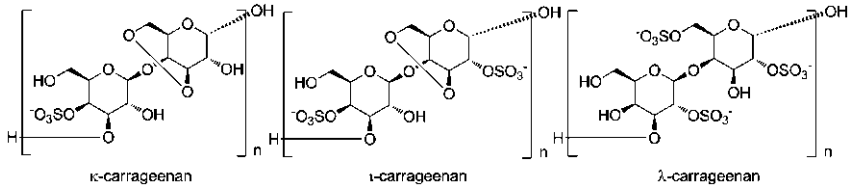

Scheme 7.3 Chemical structures of κ, ι, and λ-carrageenan.

relatively homogeneous κ-carrageenan can be obtained. *Eucheuma denticulatum* (syn. *spinosum*) is the most important source of ι-carrageenan, whereas *Gigartina pistillata* and *Chondrus crispus* mainly produce λ-carrageenan [39].

The gelling properties of the carrageenans strongly differ between the subtypes. κ-carrageenan gives strong and rigid gels, ι-carrageenan makes soft gels, and λ-carrageenan does not form gel. The gelation of a carrageenan solution is induced by cooling a hot solution that contains gel-inducing cations such as K^+ (κ-carrageenan) or Ca^{2+} (ι-carrageenan). The Na^+-form of the carrageenans does not yield a gel [39]. Detailed information on the gelling properties of the carrageenans is summarized in a recent review by Rinaudo [1].

A variety of carrageenan-degrading enzymes (carrageenase) was isolated until now. Most carrageenases are κ or ι-carrageenases, cleaving the polymeric chain of κ or ι-carrageenan in the β-glycosidic bond and yielding a di- or tetrasaccharide with a terminal 3,6-anhydrogalactose [39–41]. As the last enzyme in this context, a λ-carrageenase was cloned from *Pseudoalteromonas bacterium*, strain CL19, which was isolated from a deep-sea sediment sample. The pattern of λ-carrageenan hydrolysis shows that the enzyme is an endo-type λ-carrageenase with a tetrasaccharide of the λ-carrageenan ideal structure as the final main product. As for the other carrageenases, this enzyme also cleaves the β-1,4 linkages of its backbone structure. Remarkably, the deduced amino acid sequence shows no similarity to any reported proteins [42]. Additionally, λ-carrageenase activity was also identified and purified from the marine bacterium *Pseudoalteromonas carrageenovora* [43].

Polysaccharides are often added to dairy products to stabilize their structure, enhance viscosity, and alter textural characteristics. Also, carrageenans are used as thickener and stabilizer in the dairy industry, for example, in the production of dairy products such as processed cheese [44]. Since carrageenan is a polyanionic structure, several applications for gels with polycationic compounds such as chitosan are published. Tapia *et al.* compared chitosan–carrageenan with chitosan–alginate mixtures for the prolonged drug release. They found that the chitosan–alginate system is better than the chitosan–carrageenan system as matrix because the drug release is controlled at low percentage of the polymers in the formulation, the mean dissolution time is high, and different dissolution profiles could be obtained by changing the mode of inclusion of the polymers. In the chitosan–alginate system, the swelling behavior of the polymers controlled the drug release from the matrix. In the case of the system chitosan–carrageenan, the high capacity of carrageenan promotes the entry of water into the tablet, and therefore, the main mechanism of drug release is the disintegration instead of the swelling of the matrix [45].

In a different context, the polyelectrolyte hydrogel based on chiotosan and carrageenan was evaluated as controlled release carrier to deliver sodium diclofenac. The optimal formulation was obtained with chitosan–carrageenan as 2:1 mixture and 5% diclofenac. The controlled release of the drug was maintained under simulated gastrointestinal conditions for 8 h. Upon crosslinking with glutaric acid and glutaraldehyde, the resulting beads were found to be even more efficient and allowed the release of the drug over 24 h [46].

In a recent study, the preparation of crosslinked carrageenan beads as a controlled release delivery system was reported. Since κ-carrageenan just allowed thermoreversible gels, a protocol for an additional crosslinking using epichlorohydrin was introduced. Low epichlorohydrin concentrations led to unstable and weak beads with uneven and cracked surfaces. An optimized crosslinker concentration resulted in smooth and stable gel beads that showed great potential for the application as delivery systems in food or pharmaceutical products [47].

7.4 Cellulose and Its Derivatives

Cellulose was first described by Anselme Payen in 1838 as a residue that was obtained after aqueous extraction with ammonia and acid-treatment of plant tissues [48]. It is a carbohydrate polymer composed of β-(1→4)-linked D-glucose.

Cellulose is one of the most common polymers because it is ubiquitous in the biomass. Its chain length depends on the origin and the treatment of the polymer. The biosynthesis of cellulose has been described in numerous reviews [49]. Besides plants as polymer source, it can also be obtained from bacterial production (see Chapter 5) or from *in vitro* synthesis. Cellulose can be produced either by enzymatic polymerization of β-cellobiosyl fluoride monomers or by chemical synthesis, for example, by cationic ring-opening polymerization of glucose orthoesters. These approaches are summarized in a review from Kobayashi *et al.* [50].

The crystal structure of cellulose has been studied intensively. Two modifications of cellulose I were discovered, varying in the character of their elementary cell, which is either triclinic or monoclinic. Cellulose II is the thermodynamically most stable structure. More solid and liquid state crystal structures of cellulose and the fibrillar morphology of the polymer are summarized in the review from Klemm *et al.* [51].

Due to its numerous hydrogen bonds, cellulose is insoluble in nearly all common solvents [52]. For this reason, several cellulose solvent systems have been explored to enable its chemical modification. LiCl–dimethylacetamide mixtures as well as tetrabutylammonium fluoride in dimethyl sulfoxide or metal containing solvents, for example, cuprammonium hydroxide, have been investigated [53]. Several chemical derivatizations of cellulose can be realized in order to use cellulose as drug deliverer or for other medical applications. An overview of these modifiable functional groups is given in Scheme 7.4. For instance, cellulose can be oxidized at different positions as well as esterified or alkylated at the primary hydroxyl group. Especially the last mentioned derivatizations lead to water- and/or organic-soluble compounds, which can be used for further modifications.

The secondary alcohol groups of cellulose can be oxidized to ketones, aldehydes, or carboxylic functions depending on the reaction conditions. The product is called oxycellulose and represents an important class of biocompatible and bioresorbable polymers which is widely used in medical applications. It is known to be hemostatic, enterosorbent, and wound-healing. Furthermore, oxycellulose can be used

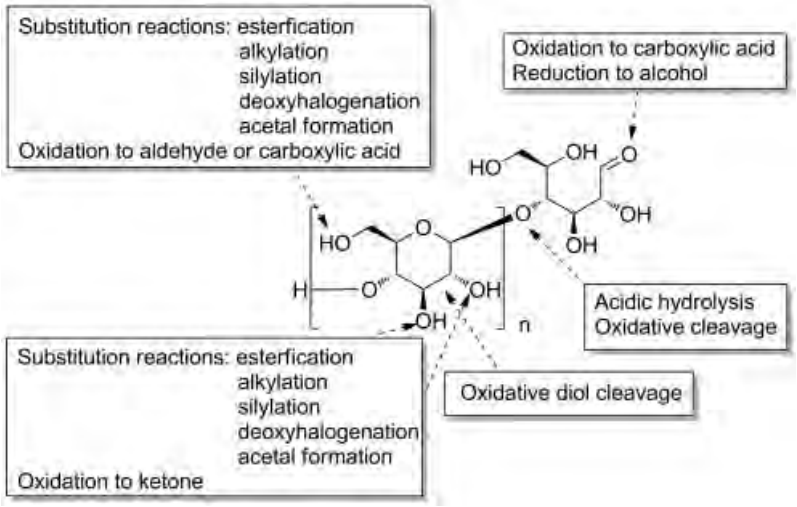

Scheme 7.4 Possible positions for chemical modification of cellulose.

as drug carrier because its carboxylic groups can be used for further derivatization, especially for the coupling of various bioactive agents such as antibiotics, antiarrhythmic drugs, and antitumor agents. By addition of these drugs to oxycellulose, their toxicity could be increased or their activity could be enhanced. For more detailed information on the synthesis and the applications of oxycellulose, see the review from Bajerová *et al*. [54]. Aldehyde-functionalized oxycellulose can be used in the field of tissue engineering. Hydrogel formation of aldehyde- and hydrazine-functionalized polysaccharides is explained in Chapter 10.

The synthesis of various cellulose esters was summarized by Seoud and Heinze [55]. They separated the functionalization process into three steps: (i) activation of the polymer by solvent, heat, or others, (ii) dissolution of the cellulose according to methods described above, and (iii) chemical derivatization. The applications of cellulose esters are multifaceted. Depending on their chemical structure, they are used as coatings for inorganic materials, laminates, optical films, and applications in the separation area such as hemodialyses and blood filtration. Several applications of cellulose esters are summarized in a review by Edgar *et al*. [56].

Another type of cellulose esters are the cellulose sulfonates, prepared from cellulose and sulfonic acid or sulfonic chloride. This class of compounds has reactive groups that can be easily substituted with nucleophilic reagents, for example, amines to yield aminocellulose, which is used as enzyme support [57].

Sodium carboxymethyl cellulose is another common cellulose derivative. This anionic, water-soluble compound is generated through etherification of the primary alcohol of cellulose. It is used as an emulsifying agent in pharmaceuticals and cosmetics [58]. Sannino *et al*. used carboxymethyl cellulose and hyaluronan hydrogels to prevent postsurgical soft tissue adhesion [59]. Both polymers were

crosslinked with divinylsulfone. Rokhade and coworkers prepared semi-interpenetrating polymer network microspheres of gelatin and sodium carboxymethyl cellulose with an encapsulated anti-inflammatory agent. Glutaraldehyde served as a crosslinker in this drug release system [60].

Silylation of cellulose with chlorosilanes or silazanes leads to thermostable silyl ethers, which are more lipophilic in comparison to unmodified cellulose. Several conditions, which lead to silyl ethers with different substitution patterns, are described in a review by Klemm *et al.* [51]

Other etherified cellulose derivatives, for example, methycellulose, ethylcellulose, hydroxypropyl cellulose, and hydroxypropyl methyl cellulose, are described elsewhere [58]. Briefly, methycellulose is used in bulk laxatives, nose drops, ophthalmic preparations, and burn ointments, and ethylcellulose has a broad range of applications because it is insoluble in water but soluble in polar organic solvents.

7.5 Microbial Cellulose

Microbial cellulose (MC) belongs to the group of homopolysaccharides, which consists of only one type of monosaccharide, in the case of MC, β-D-glucose. The monomers are linked through 1→4 glycosidic bonds (Scheme 7.5).

The production of MC was first observed by A. J. Brown in 1886, who found out that cellulose was produced in resting cells from *Acetobacter xylinum* in the presence of oxygen and glucose [61]. Other bacteria which produce MC are *Agrobacterium*, *Acetobacter*, *Aerobacter*, *Archromobacter*, *Azotobacter*, *Rhizobium*, *Sarcina*, and *Salmonella*. The review from Chawla *et al.* gives an overview concerning the cultivation conditions of the different strains [62]. The fermentation process and the biosynthesis for MC are in-depth described in recent published reviews [63, 64]. Briefly, the complex process consists of three steps; namely: (i) the linear strand formation from uridine diphosphoglycose, catalyzed by cellulose synthetase, a membrane-anchored protein, (ii) the extracellular secretion of the chain, and (iii)

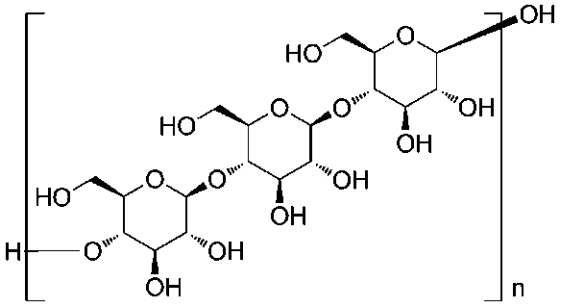

Scheme 7.5 Chemical structure of cellulose.

assembly to hierarchically composed ribbon-shaped microfibrils of approximately 80×4 nm [65].

Although it has the same chemical structure as plant cellulose, the MC can be obtained in higher purities and it has a higher degree of polymerization and crystallinity. The fibrils of bacterial cellulose are 100 times thinner than their plant analogs. Furthermore, it has remarkable water-holding capacity and a high tensile strength, which results from the interfibrillar hydrogen bonding. These physical properties made MC to a promising candidate for biomedical applications.

Besides the physical properties described above, MC has a lot of advantages in the wound-healing process. Due to its nanoporous structure, external bacteria cannot penetrate the wound. It is easy to sterilize, cheap, and elastic which provides a painless wound coverage and removal. The material is highly porous and allows an unhindered gas exchange [66]. Helenius *et al.* evaluated the bacterial cellulose in aspects of chronic inflammation, foreign body responses, cell ingrowth, and angiogenesis [67]. MC proved to be entirely biocompatible. This is why MC is often used as wound dressing material, which protects the wounds from infection or dehydration. The review from Czaja *et al.* summarized the application of MC in the field of wound treatment [68]. Several approaches have been made to improve and accelerate the healing process, for example, by impregnation of the MC tissue with therapeutic agents such as superoxide dismutas or poviargol [69]. Additionally, several composites with other polymers such as gelatin have been reported [70].

MC is also used as tissue material in artificial cardiovascular medicine. Therefore, it is necessary to mold the polymer into the needed shape during its synthesis. Different techniques for this demand are summarized elsewhere [51, 66]. Charpentier *et al.* published another approach in the exploration of a vascular prosthetic device. They used PETG and PCTG polyesters as backbone material, modified the surface with UV and plasma treatment and coated it with MC to reduce coagulation effects of the material [71].

Another patented system deals with the coating of endoprostheses with MC, in order to obtain biocompatible devices [72]. MC is also used as physical barrier, which separates bone cells from the surrounding tissue to prevent fibroblast cell ingrowth. This accelerates the regeneration process of the osseous cells [73, 74]. MC was tested as a 3-D scaffold for *in vitro* cell cultivation to mimic the extracellular matrix. Afterward, the overgrown tissue should be implanted into the body to replace the diseased area [75].

7.6 Chitin and Chitosan

Chitin and chitosan are structurally related aminopolysaccharides. Both polysaccharides may be regarded as derivatives of cellulose, where chitin bears an acetamido group and chitosan bears a aminogroup instead of the C-2 hydroxyl functionality (Scheme 7.6).

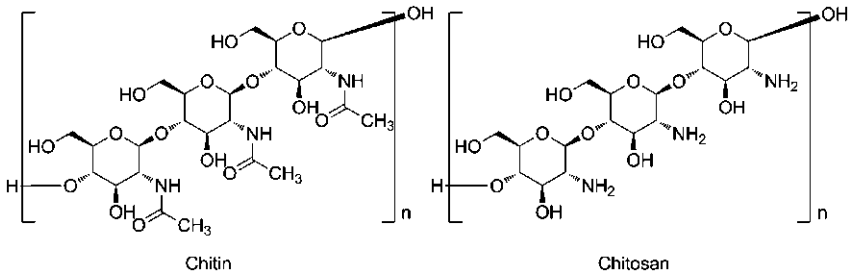

Scheme 7.6 Chemical structures of chitin and chitosan.

Chitin is the second most abundant biopolymer after cellulose and is found in ordered fibrils in cell walls of fungi and yeast and in the exoskeleton of crustaceans and insects. The main commercial sources of chitin are shrimp and crab shells, a waste product of the seafood production. For the production of pure chitin, the shells are deproteinized under basic conditions and subsequently demineralized under acidic conditions to remove $CaCO_3$. It is important to note that chitin shows three different crystalline structures depending on its function in nature. The outer skeletal chitin in crustaceans consists of α-chitin, squid pen consists of β-chitin, and fungi contain γ-chitin. Chitin shows a high biocompatibility, an excellent biodegradability, and a low immunogenicity. A major problem is the low solubility of chitin in water and almost all common organic solvents due to its high crystallinity [76]. *N*-deacetylation in concentrated alkali solution at high temperatures or using the enzyme chitin deacetylase (EC 3.5.1.41) leads to chitosan. The chemical *N*-deacetylation can be performed in two different ways. In a heterogeneous process, chitin is treated with 10–60% sodium hydroxide solution at 70–150 °C for up to 6 h. Chitosan prepared by this method is approximately 90% deacetylated [77]. A milder homogenous process leads to water-soluble chitosan which is 50% deacetylated by storing an alkaline solution of chitin for 77 h at room temperature [78]. The predominant thermochemical chitosan production is environmentally unsafe and hard to control, leading to broad range of products with a lower molecular mass due to partial hydrolysis of the polymeric chain. The use of chitin deacetylase (ED 3.5.1.41), which could be isolated and cloned from various fungi and insects, can circumvent some of these problems. It was shown that a 97% deacetylation of chitosan is possible using partially deacetylated chitosan as substrate. The enzymatic deacetylation of crystalline or amorphous chitin is still less effective yielding a 0.5–9.5% deacetylated product [79]. Naturally occurring chitosan is very rare and can be found together with chitin in several fungi. Since chitosan is rare, chitosan-degrading enzymes are less abundant. Lysozyme does also, in addition to its natural substrate (the glycosidic linkage of certain bacterial cell walls peptidoglycans), hydrolyze chitin and chitosans. Lysozyme is present in many tissues and secretions such as tears, saliva, and blood [80, 81]. In a detailed study, the enzymatic (lysozyme, chitinase, etc.) digestibility of various

chitins and chitosans was investigated. It turned out that the digestibility of chitin by the chitinase from *Bacillus* sp. PI-7S is much higher than by lysozyme. Also β-chitin was digested more smoothly than α-chitin, and chitosan deacetylated under homogeneous conditions was hydrolyzed by lysozyme more rapidly than that under heterogeneous conditions [82].

In contrast to chitin, chitosan is highly soluble in diluted acids. The primary amino groups in chitosan are protonated below pH 6.0, resulting in a water-soluble cationic polyelectrolyte. At higher pH values, the ammonium salt gets deprotonated resulting in a neutral amino group and the polymer gets insoluble. On the other hand, this solubility transition is highly dependent on the degree of *N*-acetylation and chitosan with 50% *N*-acetylation is soluble even under alkaline conditions [78]. In addition, the anion of the acid plays an important role for the solubility of chitosan. While many acids such as acetic, citric, formic, hydrochloric, lactic, and diluted nitric acid can easily dissolve chitosan, the phosphates and sulfates of chitosan are not soluble in water [76].

Several approaches were published to solubilize chitin with and without chemical modification of the polymer. 2.77 M sodium hydroxide was reported as good solvent for chitin and the addition of urea did improve the solubility [83]. A powerful organic solvent system for chitin was first described by Austin and Rutherford. They found that lithium chloride forms a complex with the acetamide carbonyl group of chitin [84]. The resulting complex is soluble in polar organic solvents such as *N*-methyl-2-pyrrolidinone, *N,N*-dimethylacetamide, *N,N*-dimethylpropionamide, and 1,3-dimethyl-2-imidazolidinone. Chitin solutions with a concentration of 5–7% (w/v) could be obtained using these conditions [85]. Another suitable solvent system is $CaCl_2$-dihydrate saturated methanol as reported by Tamura [86]. The water content is essential and anhydrous $CaCl_2$ in methanol does not dissolve chitin at all. Two grams of α-chitin powder can be dissolved in 100 mL of $CaCl_2 \cdot (H_2O)_2$-saturated methanol but just 0.5–1 g of β-chitin is soluble under those conditions. The solubility is also affected by the degree of *N*-acetylation and the molecular weight of chitin as depicted in Figure 7.1 [87].

Another successful strategy for chitin dissolution is the synthesis of soluble chitin esters. The introduction of bulky acyl groups into the chitin chain yields chitin derivatives with improved solubility [88]. Acetylchitin is readily synthesized and spun into fibers but still polar acidic solvents such as formic acid are necessary to dissolve the material [89]. Butyrylchitin, with a larger substituent in the chain, can be synthesized using methanesulphonic acid as catalyst and solvent. This derivative is easily soluble in several organic solvents, such as acetone, methanol, ethanol, dimethylformamide, and methylene chloride [90]. A simpler method for the synthesis of highly substituted dibutyrylchitin with butyric anhydride uses 70% perchloric acid as a catalyst. Dibutyrylchitin fibers with a porous core were made by a simple method of dry spinning its 20–22% solutions in acetone. These fibers have tensile properties similar to or better than those of chitin. Alkaline hydrolysis of the butyric esters restores chitin, and even fibers with good tensile properties can be obtained by alkaline hydrolysis of dibutyrylchitin fibers in 5% sodium hydroxide at 55 °C without destroying the fiber structure [91]. The ester cleavage

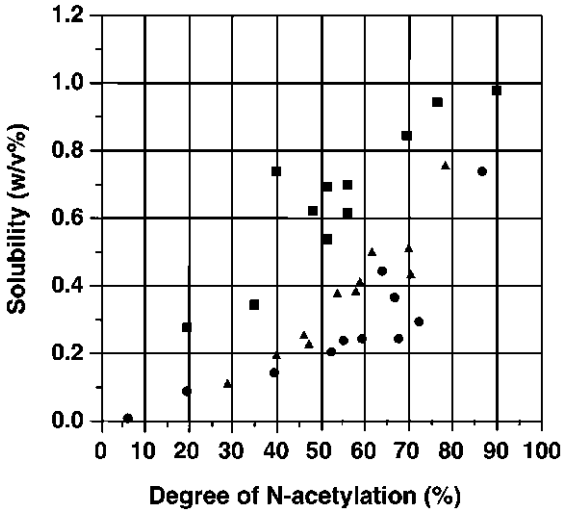

Figure 7.1 Dependence of the $CaCl_2$-dihydrate/methanol solubility of chitin with respect to the degree of acetylation and the molecular weight of chitin. Solid square, 1.2×104; solid triangle, 4.0×104; solid circle, 1.6×105 (with permission from Ref. [87]).

can be monitored by FTIR spectroscopy and by the weight loss of the material, which raised up to 40% for a complete hydrolysis. The restoration of the chitin structure from dibutyrylchitin fibers resulted in an increase of the degree of crystallinity and in the diameter of the fibers along with a decrease of the tensile strength [92].

The peculiar biochemical properties of chitins and chitosans remain unmatched by other polysaccharides. The major areas of application include water treatment, biomedical applications (including wound dressing and artificial skin), and personal-care products. Chitin and chitosan-based materials have unique characteristics in the area of tissue regeneration. Hemostasis is immediately obtained after application of chitin-based dressings to traumatic and surgical wounds: platelets are activated by chitin with redundant effects and superior performances compared with known hemostatic materials. To promote angiogenesis, the production of the vascular endothelial growth factor is upregulated in wound healing when macrophages are activated by chitin/chitosan. Biocompatible wound dressings derived from chitin are available in the form of hydrogels, xerogels, powders, composites, films, and scaffolds. The scaffolds are easily colonized by human cells to restore tissue defects. Chitin tubes, which can be manufactured from the tendon of the crab leg muscle or by using electrospun chitosan nonwoven, can be implanted to bridge a dissected nerve and used as alternative to autologous grafts. Chitosan is also used in cartilage tissue engineering where it provides an environment in which the chrondrocytes maintain their correct morphology and their capacity to synthesize the correct extracellular matrix. Scaffolds made of either pure β-chitin, or pure chitosan, or mixtures of both polysaccharides had the same

efficiency in supporting chondrocytes. Chitosan composites can also be used in the treatment of bone defects, where it promotes growth and mineral-rich matrix deposition by osteoblasts. Especially, porous hydroxyapatite–chitin matrices have a great potential in this field of regenerative therapy [93].

7.7 Dextran

Dextran belongs to the family of homopolysaccharides, precisely to the complex, multibranched glucans. Glucans are polysaccharides which are built up by glucose monomeric units. Dextran itself is constructed by a specific form of glucose, α-D-glucopyranose. The polymeric chain consists of a substantial number of consecutive α-(1→6) linkages in their major chains, usually more than 50% of the total linkages. Further side chains result mainly from α-(1→3) and occasionally from α-(1→2) or α-(1→4) linkages. Overall the molecular weight differs from 10 to 150 kDa (Scheme 7.7).

The exact network of a specific dextran depends on its individual producing microbial strain. Dextran is produced either in *Leuconostoc mesenteroides* and other lactic acid bacteria or in certain *Gluconobacter oxydans*. The former converts sucrose into dextran with the dextransucrase enzyme, whereas the latter converts maltodextrins into dextran with the dextran dextrinase enzyme [94]. The enzyme dextransucrase catalyzes the transfer of D-glucopyranosyl moieties from sucrose to dextran, while fructose is released. Thereby dextransucrose acts substrate specific because other native saccharides like fructose, glucose, or mixtures of both are not converted. Furthermore, no adenosine triphosphate or cofactors are required [95]. According to the classification of transferases, dextransucrase is an extracellular glucosyltransferase. Until today, more than 30 sucrose glycosyltransferase genes have been sequenced and their catalytic sites have been identified. The families of glycosyltransferases and glycoside-hydrolases share related mechanistic and structural characteristics [96].

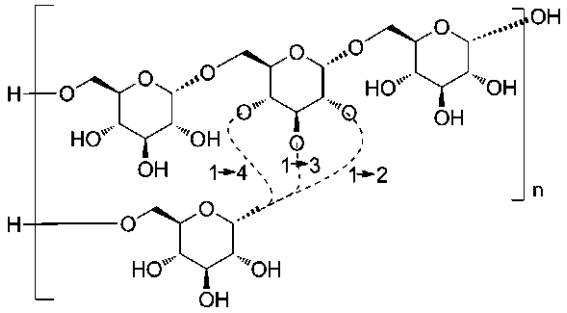

Scheme 7.7 Chemical structure of dextran with exemplary α(1→2), α(1→3), and α(1→4) linkages.

The synthesis of unbranched dextran was already published in the 1950s [97]. Nowadays, dextran can also be synthesized via cationic ring-opening polymerization of 1,6-anhydro-2,3,4-tri-*O*-allyl-β-D-glucopyranose [98]. Commercially available dextran is generally produced by dextransucrase NRRL B-512F from *L. mesenteroides*. In this process, cultures of *L. mesenteroides* were grown in sucrose-containing media with growth factors, trace minerals, and an organic nitrogen source. In former times, Naessens *et al*. have shown that forms of *G. oxydans* could be a promising alternative to *L. mesenteroides* as biocatalysts for the synthesis of dextran and oligodextrans [99].

Dextran is enzymatically degraded by dextranase into dextrose (D-glucose). Dextranases belong to the family of glycosyl-hydrolases and are subdivided into endo- and exodextranses (Figure 7.2). In organisms, these enzymes are present in human liver, intestinal mucosa, colon, spleen, and kidney. Since the first reports on *Cellvibrio fulva* dextranase in the 1940s, more than 1500 scientific papers and more than 100 patents have been issued on dextran-hydrolyzing enzymes found in a number of microbial groups, fungi being the most important commercial source of dextranase [100, 101]. Enzymatically fractionated dextran with a specific chain length and individual characteristics possesses interest in different branches of industry. It can be implemented in cosmetics, drug formulations, and vacancies, as cryoprotectants, and as stabilizers in the food industry.

In general, derivatization occurs at the hydroxyl groups in the monomeric unit. Several approaches for crosslinking dextran are published. Bis-acrylamid, epichlorhydrin, diisocyanates, phosphorus oxychloride, methacrylate, acylate, and other functions were favored. In addition, esterifications by inorganic or organic compounds have been established. In the range of inorganic ester, only the sulfates and the phosphates have gained interest. The introduction of these ionic groups leads to polyelectrolytes with an improved water solubility. In contrast to the broad

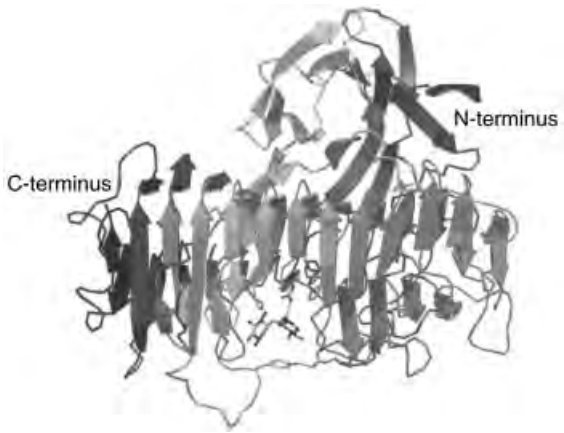

Figure 7.2 Crystal structure of endodextranase Dex49A from *Penicillium minioluteum* with isomaltose in the product-bound form (with permission from Ref. [101]).

variety of applications of 1→4- and 1→3-linked glucans after reaction with (C-2 to C-4) carboxylic acid anhydrides and chlorides, the use of dextran esters of short-chain aliphatic acids such as acetates or propionates is rather limited. Moreover, several ether derivatives were established. A detailed overview about the chemistry, biology, and application of functional polymers based on dextran is given by Heinze *et al*. [102].

For medical usage, dextran has many useful characteristics. It is highly biocompatible, slowly degraded, innocuous to the body and readily excreted from it. Hence, dextran has found application in clinic; especially, biodegradable dextran hydrogels are widely used for protein delivery [103], due to the fact that they can act as carriers for a controlled release of drugs to targeted organs mediated by slow dextranase hydrolysis. Kim *et al*. have presented the *in vitro* drug release behavior of dextran–methacrylate hydrogels using doxorubicin [104]. A recent publication has shown that injectable *in situ* crosslinking hydrogels by hydrazone formation can be used for local antifungal therapy [105]. Mostly aqueous solutions of dextran are used as blood volume expander [106]. This relies to the feature that a 6% dextran solution with an average molecular mass of about 75 kDa provides an osmotically neutral fluid comparing to the blood. Molecules with a too low molecular weight are removed rapidly from the blood circulation via the kidneys, whereas molecules with a too high molecular weight can interfere with the normal coagulation process. Furthermore, 40 kDa dextran improves the blood flow besides the plasma volume expansion, presumably mediated by reduction of blood viscosity and inhibition of erythrocyte aggregation [107].

In a further application, crosslinked dextran chains are often used as purification and/or separation material. Epichlorohydrin crosslinked dextran forms a gel which is used as release agent. A most common separation process to fractionate water-soluble substances by molecular size is Sephadex®. Elementary Sephadex, derived from SEparation PHAmarcia DEXtran, gels are prepared by crosslinking dextran to a macromolecular network of great stability [108].

Dextrans and derivatives are widely used in nutrition products, fructose syrup, and as additives in bakery, candies, and ice cream. Moreover, it has upraising potential uses as emulsifying and thickening agents, high-viscosity gums, explosives, deflocculants in paper industry, oil drilling muds, soil conditioners, and surgical sutures [109]. An interesting approach is the introduction of dextranases for the degradation and removal of dental caries. Dental plaque consists of ~20% glucans; consequently, dextranses could inhibit the synthesis of insoluble glucans [110].

7.8 Gellan

Gellan is a linear anionic bacterial exopolysaccharide with a repeating unit based on the tetrasaccharide → 3)-D-glucopyranosyl-β-(1→4)-D-glucuronopyranosyl-β-(1→4)-D-glucopyranosyl-β-(1→4)-L-rhamnopyranosyl-α-(1→3). In its native form,

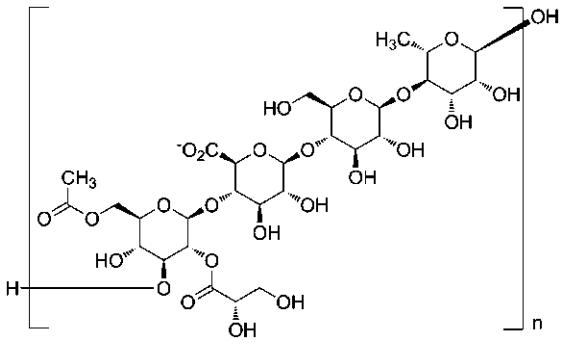

Scheme 7.8 Chemical structure of high-acyl gellan.

gellan bears an acetyl group at position 6 and an L-glyceryl group at position 2 of the glucose β-(1→4) linked to the glucuronic acid. It consists of about 50,000 sugar units and is normally deacylated before use [111] (Scheme 7.8).

Gellan gum is produced via submerged fermentation using *Sphingomonas paucimobilis* ATCC 31461. Studies on the nutritional requirements for optimal exopolysaccharide production in a salt-based synthetic medium reveal soluble starch (20 g/L) as the best carbon source and tryptone (0.5 w/v%) as the best nitrogen source. A maximum of 35.7 g/L gellan is produced under optimized conditions. After heating the crude fermentation broth at pH 10, deacetylated gellan can also be isolated by precipitation [112].

Under suitable conditions, the native gellan gum forms soft, elastic, transparent, and flexible gels. In contrast, the deacylated gellan forms stiff and brittle gels in the presence of many cations such as Ca^{2+}, Mg^{2+}, Na^{+}, K^{+}, and H^{+} [113]. Physical properties such as the setting temperature, strength, and firmness of the gel depend on the type of cation used for the gelation, as well as its ionic strength. For example, potassium ions set the gels at a lower temperature than calcium ions. In contrast, calcium ions can yield gels of the same strength and quality as potassium, but at a much lower concentration of 1/40th that of the monovalent ions. The X-ray-based solid phase tertiary structure of deacylated gellan was reported by Chandrasekaran *et al.* to consist of two identical left-handed, threefold double helices [114]. The molecular origin for rheological characteristics of native gellan gum is discussed by Tako *et al.* The ^{1}H-nuclear magnetic resonance spectra of gellan in its native and deacylated form show that the L-rhamnosyl residues of native gellan involved a small number of $^{4}C_{1}$-pyranose conformations and a large number of $^{1}C_{4}$-pyranose conformations, whereas for deacylated polymer, almost all of the residues were involved in $^{4}C_{1}$-pyranose conformation [111]. Such conformational changes of the L-rhamnosyl residues contribute to the gel formation for deacetylated rhamsan gum which is effectively a gentiobiosylated form of gellan [115].

In a broad screen, Gellan was found to be degradable by a number of bacterial strains identified as *Bacillus* sp. Several Gram-negative bacteria secrete extracel-

lular eliminase-type enzymes (lyases) which are cleaving the sequence β-D-glucopyranosyl-β-(1→4)-D-glucuronopyranosyl in the tetrasaccharide repeat unit of gellan. In most of the bacterial isolates, the lyases are predominantly endoenzymes. The enzymes are highly specific toward gellan and rhamsan but do not degrade most of the other bacterial exopolysaccharides, which are structurally related to gellan [116, 117]. Hashimoto *et al*. cloned a 140 kDa gellan lyase from *Bacillus* sp GL1. The recombinant enzyme is most active at pH 7.5, 50 °C and stable below 45 °C. The recombinant lyase is active on gellan, especially in the deacylated form, but is inert against gellan-related polysaccharides such as S-88, welan, rhamsan, and S-198 [118].

A thermostable gellan lyase, with a residual activity of 100% after 24 h incubation at 60 °C and a half-life time of 60 min at 70 °C, was isolated form a thermophilic strain *Geobacillus stearothermophilus*. The strain produces the thermostable gellan lyase extracellularly during exponential phase and the enzyme is not present in culture liquid without gellan. The enzyme has an optimal activity at 75 °C in a very large pH area between 4 and 8.5 [119].

The easiest and most common modification of gellan is the complete deacylation. The native gellan gum is dissolved in 0.2 M potassium hydroxide and stirred at room temperature for 12 h under atmosphere of nitrogen. After neutralization with 0.1 M hydrochloric acid and filtration through Celite 545, the deacylated gellan can be precipitated in the presence of 0.05% KCl by the addition of two volumes ethanol [111].

In a recent study, acrylate and maleate esters were synthesized. The esterfication is possible using homogenous (acrylic acid in water) or heterogeneous (acryloyl chloride or maleic anhydride in *N,N*-dimethylformamide or aceton) reaction conditions. These macromonomeres can be polymerized under mild conditions and lead to biodegradable thermo- and pH-stimulable hydrogels with adjustable crosslink density [120].

Self-crosslinking of aqueous gellan with 1-ethyl-3-[3-(dimethylammino)propyl]-carbodiimide leads to thermally stable hydrogels. Based on X-ray data, the structure of the gel is proposed to be a bundle of 48 gellan double helices aligned in parallel. The rigid bundles formed by associated gellan double helices constitute the junction zones which sustain the overall gel structure displaying solid-like properties. Relatively large cavities supported by rigid bundles inside the gels absorb water quickly as indicated by kinetic water uptake data [121].

Gellan was approved for use in food in Japan in 1988 and in the United States in 1992. Today gellan is used in food products, which require a highly gelled structure such as meat and vegetable aspic, jams, and jellies. As an example, reduced calorie jams can be prepared with only 0.15% of clarified gellan, and a matrix containing 0.7% gellan does not melt on sterilization. In addition, gellan is used to provide body and mouth-feel as a substitute of gelatin and to speed up the set time of jellies as a substitute of starch.

Additionally, gellan is used as solid culture media for growth of microorganisms and plants, as matrix in gel electrophoresis and to immobilize cells. Gellan has some promising properties in the area of controlled drug release. Sustained

delivery of paracetamol from gels formed *in situ* in the stomach is similar to commercially available suspension. Also, gellan-based ophthalmic solutions are reported to have longer residence time in tear fluid than saline solution. In both applications, the solution of gellan mixed with drugs *in situ* forms a gel at acidic pH in the stomach or in the presence of ions in the lachrymal fluid [122].

In a first study to evaluate gellan as scaffold material for tissue engineering, gellan could be ionically crosslinked on mixing with α-modified minimum essential medium resulting in the formation of a self-supporting hydrogel. By adding a suspension of rat bone marrow cells in α-modified minimum essential medium to 1% gellan solution, it is possible to immobilize cells within the three-dimensional gellan matrix that remain viable for up to 21 days in culture. This simple approach to cell immobilization within three-dimensional constructs poses a low risk to a cell population immobilized within a gellan matrix and thus indicates the potential of gellan for use as a tissue engineering scaffold [123].

7.9 Guar Gum

Guar gum belongs to the group of galactomannans and is a neutral polysaccharide with a main chain composed of β-(1→4)-linked mannose units and a molecular weight of approximately 1×10^6 Da. On average, every second mannose is substituted at position 6 with a α-D-galactopyranose. Analysis of the products obtained by enzymatic digestion indicates that in guar galactomannan, the D-galactosyl groups are arranged mainly in pairs and triplets [124] (Scheme 7.9).

Guar gum is isolated from the seed of *Cyamopsis tetragonoloba*, which belongs to the Luguminosoe family. Guar gum forms crosslinked hydrogels on treatment with borax or calcium ions. However, its aqueous solution is nonionic and hydrocolloidal and is not affected by ionic strength or pH. In order to yield a monodisperse guar gum fraction, a purification procedure modified by Wientjes *et al.* can

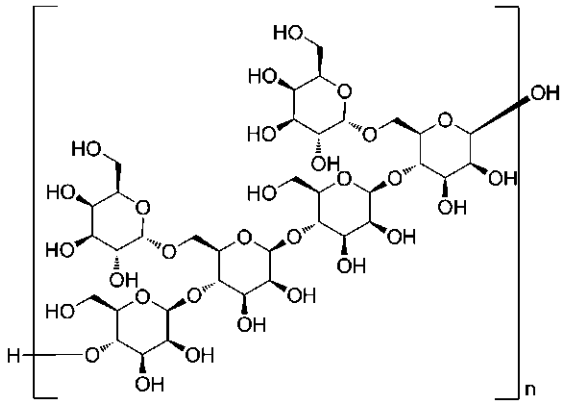

Scheme 7.9 Chemical structure of guar gum.

be applied: Crude guar gum (10 g) is treated with 200 mL boiling, aqueous 80% ethanol for 10 min. The obtained slurry is collected on a glass filter (no. 3) and washed successively with ethanol, acetone, and diethyl ether. The solid is added to 1 l of water, homogenized with a blender, and centrifuged at 2300 g for 15 min. The supernatant is precipitated in two volumes of cold acetone, redissolved in hot water, and ultracentrifuged at 82,000 g for 1.5 h at room temperature. Finally, the supernatant is precipitated with two volumes of ethanol and precipitate is collected on a glass filter (no. 4), washed with ethanol, acetone, and diethyl ether before freeze-drying [125].

Three kinds of bonds in guar gum are susceptible to enzymatic hydrolysis: the endo- and exo-β-1,4 linkages on the D-mannose backbone and the α-1,6 linkage between the mannose backbone and the galactose side chain. The enzymes that cleave these bonds are, respectively, endo- and exo-β-mannanase and α-galactosidase [126]. The 1,4-β-D-mannosidic linkages in galactomannans can be hydrolyzed by β-D-mannanases, a class of enzymes which is produced by plants, bacteria, and fungi. The efficiency of this reaction depends both on the degree of polymerization and galactose substitution levels [127]. Galactomannans with a galactose content of up to 32% are hydrolyzed with no significant change of the K_m or relative V_{max} values. However, if the galactose content approaches 34–38%, the K_m values doubles, and the relative V_{max} values decreases by 10–20%. Typically, 6% of the mannosidic linkages in guar gum are hydrolyzed [128]. Since galactomannans as guar gum are used in hydraulic fracturing of oil and gas wells, it is necessary to employ thermostable enzymes for the enzymatic degradation. Commonly applied enzymatic breakers are mixtures of hemicellulases produced by *Aspergillus niger*. This enzyme preparation is moderately thermostable with temperature optima of approximately 65 °C and it has shown to be effective for galactomannan hydrolysis and viscosity reduction. McChutchen *et al*. isolated and characterized a α-galactosidase and a β-mannanase produced by the hyperthermophilic bacterium *Thermotoga neapolitana* 5068. The purified α-galactosidase had a temperature optimum of 100–105 °C with a half-life of 130 min at 90 °C and 3 min at 100 °C. The purified β-mannanase was found to have a temperature optimum of 91 °C with a half-life of 13 h at that temperature and 35 min at 100 °C [129].

To yield derivatives with adjusted material properties, guar gum can be carboxymethylated by the reaction with the sodium salt of monochloroacetic acid in presence of sodium hydroxide. Using homogenous reaction conditions, various degrees of substitution can be synthesized. Aqueous solutions of carboxymethylated guar gum have higher viscosities compared to unmodified guar gum [130]. Another important derivative is hydroxypropyl guar gum, a hydrophobic polymer obtained from the native biopolymer via an irreversible nucleophilic substitution, using propylene oxide in the presence of an alkaline catalyst. When guar gum is modified to hydroxypropyl guar, the added hydroxypropyl groups sterically block the hydrogen bonding sites on the guar backbone and reduce the hydrogen-bonding attractions between guar molecules. In comparison to guar gum, this derivative has an improved viscosity [131].

Several protocols are published describing the synthesis of grafted guar gum [132]. Nayak and Singh described the ceric-ammonium-nitrate-initiated graft copolymerization of polyacrylamide onto hydroxypropyl guar gum by solution polymerization technique. Six grades of graft copolymers have been synthesized by varying catalyst and monomer concentrations. The percentage of grafting increases with increasing catalyst concentration and decreases with monomer concentration taking other parameters constant [133].

Native and modified guar gum is widely used in petroleum industry as additives in aqueous fracturing fluids and in drilling shallow wells. These applications utilize the properties to increase viscosity, reduce fluid loss, and decrease fluid friction. Additionally, several applications were published using guar gum in the field of controlled drug release and drug delivery. Soppirnath and Aminabhavi prepared a graft copolymer of guar gum with acrylamide, which was crosslinked with glutaraldehyde to form the hydrogel microspheres by the water-in-oil emulsification method. The microspheres were loaded with two antihypertensive drugs, verapamil hydrochloride (water-soluble) and nifedipine (water-insoluble) to investigate their controlled release characteristics. The drugs could be incorporated either during crosslinking by dissolving it in the reaction medium or after crosslinking by the soaking technique [134]. The synthesis of acryloyl guar gum and its hydrogel materials for use in the slow release of L-DOPA and L-tyrosine is described by Thakur *et al.* The material obtained has good properties as release devices for transdermal applications for the treatment of diseases like vitiligo and Parkinson's disease. The hydrogels exhibit unique swelling behavior, and respond well to the physiological stimuli such as pH and the ionic strength. A high loading capacity of L-tyrosine and L-DOPA and a slow release behavior – especially at pH 7.4 – was achieved with these hydrogel materials [135].

Tiwari *et al.* reported the synthesis of biodegradable hydrogels-based photopolymerized guar gum-methacrylate macromonomers for *in situ* fabrication of tissue engineering scaffolds. Depending on the reaction conditions, the hydrogels exhibit equilibrium swelling ratios between 22% and 63%. The degree of β-D-mannanases-induced biodegradation of the hydrogels decreased linearly with increasing gel content and the degree of methacrylation of the respective macromonomers [136].

7.10 Hyaluronic Acid (Hyaluronan)

Hyaluronic acid (HyA) is a linear, high molecular weight polysaccharide composed of β-(1→4)- and β-(1→3)-linked *N*-acetyl-D-glucosamine (GlcNAc) and D-glucuronic acid (GlcA) (Scheme 7.10). This polysaccharide was discovered in 1934 by Meyer and Palmer in the vitreous humor of cattle eyes [137]. Eponymous for the polymer was the Greek word "halos," which stands for glass, in combination with its component "uronic acid." In 1986, HyA was renamed hyaluronan due to the inter-

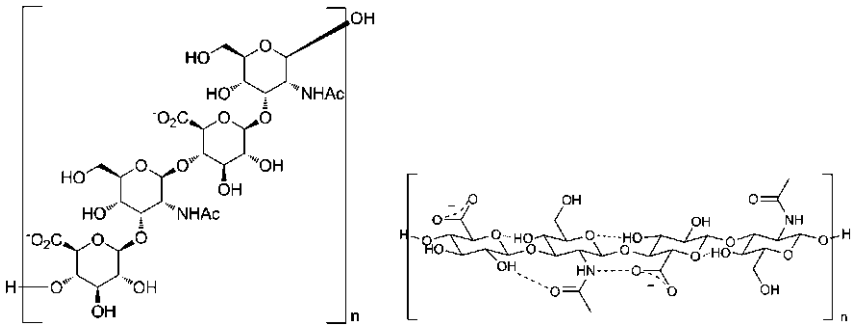

Scheme 7.10 Chemical structure of hyaluran; the dotted lines represent proposed hydrogen bonds.

national nomenclature of the IUPAC commission [138]. This name pays attention to the fact that hyaluronan has a polyanionic structure with a range of corresponding cations, for example, Na^+,K^+, and H^+.

Scheme 7.10 also shows the possible hydrogen bonds (dotted lines) of a HyA tetrasaccharide in dimethyl sulfoxide. If the polymer is solved in water, the solvent molecules are bonded between the carboxylic group of D-glucuronic acid and the amide nitrogen of *N*-acetyl-D-glucosamine. As a consequence, HyA can store large amounts of water and is highly viscous in aqueous solutions. By dissolving the HyA in alkaline solutions, a drastic decrease in the viscosity can be observed due to the deprotonation of the hydroxyl groups, which are involved in the hydrogen bonding in neutral solutions. The secondary structure of HyA was reviewed by Lapčik and Hargittai [139, 140].

Hyaluronan is synthesized by hyaluronan synthetases and can mainly be found in connective tissue, for example, in vitreous fluid of eyes, in synovial fluid, or in chicken combs [141]. The lowest concentrations were detected in blood serum. Nowadays, most of the commercially available HyA for synthetic applications is produced by bacteria, for example, by *Streptococcus equi* and *S. zooepidemicus* yielding about 4 g of HyA from 1 l, cultivation broth [139]. Unfortunately, this fermentative HyA production method bears the risk of mutations of the bacterial strains and the coproduction of toxins [142]. The analysis of HyA with electrophoretic and chromatographic techniques regarding its molecular size is reviewed by Kakehi *et al.* [143].

The biological function of HyA in the body of verbrates is dependent on the chain length of the polymer. High-molecular-weight polymers (4×10^2 to 2×10^4 kDa) are space-filling, antiangiogenic, immunosuppressive, and impede the cell differentiation, while smaller polymers play a role in ovulation, embryogenesis, protection of epithelial integrity, and wound healing as well as regeneration processes. Small oligosaccharides are inflammatory, immunostimulatory, angiogenic, and can be antiapoptotic [144].

HyA is degraded by hyaluronidases (Hyals), a very heterogeneous class of enzymes concerning their mode of action and their optimal working conditions [145]. Besides HyA, the Hyals also accept chondroitin and chondroitin sulfates as substrates. Karl Meyer separated the Hyals in three classes and his classification is still up to date [146, 147].

1) Vertebrate endo-β-*N*-acetyl-hexonaminidases, which hydrolyzes the substrate.
2) Bacterial Hyals (β-eliminases), which eliminates the glycosic linkage through introduction of a double bond.
3) A group of little explored endo-β-glucuronidases from leeches, whose mode of action resembles the verbrate Hyals.

In a vertebrate body, HyA has a very high turnover rate of about 5 g a day resulting in a half-life in the bloodstream of 2–5 min. HyA is not only degraded by Hyals but also in a catabolic pathway initiated by reactive oxygen species such as hydroxyl radicals [148]. The excretion of HyA is described in the review from Lebel [149].

The clinic applications of HyA were summarized and classified by Balazs in 2004 [142, 150].

1) **Viscosurgery:** HyA is used to protect damaged tissues and provide space during ophthalmological surgeries. Because HyA is one of the major components in the vitreous fluid of the eye, due to its viscoelastic properties, it has to be replaced, when it is lost during the extraction or replacement of damaged lenses. These surgeries are necessary after a cateract, for example, caused by diabetes mellitus. The first product on the marked for this application was Healon (noninflammatory fraction of Na-hyaluronate), produced by Biotrics, Inc., Arlington, MA and later by Pharmacia, Uppsala in Sweden.

2) **Viscoprotection:** HyA can protect healthy or wounded tissue from dryness. Healon is used to moisten the eyes pupils, although HyA is not present in tears. The advantage is that the polymer is not removed while blinking.

3) **Viscosupplementation:** HyA can be applied intra-articular, if the synovial fluid is damaged by osteoarthritis, which leads to stiff and painful joints. This disease affects about 10% of the world's population and is particular common for older people. By injecting high-molecular-weight HyA in the joint fluid, viscoelasticity increases and the production of endogenous HyA is stimulated. This is necessary because the content and molecular weight of naturally produced HyA is reduced in the patient. Additionally, inflammatory mediators are inhibited and cartilage degradation is decreased. For this application, several products containing HyA are on the marked [147].

4) **Viscoaugmentation:** HyA also fills spaces in skin, sphincter muscles, vocal, and pharyngeal tracts, and this is why, it is used in the therapy of injured tissue in the field of otolaryngology. Its shock absorption, wound healing, and osmotic functions play an especially important role in the vocal folds, due to the constant trauma caused by vibratory actions of phonation [150].

5) **Viscoseparation:** HyA is used to inhibit adhesion between two surgically traumatized tissue surfaces.

The problem with HyA containing products for the application described before is the short half-life time of the polymer, which leads to numerous repetitions of the medical treatment. Therefore, several attempts have been made to crosslink the HyA single strands to create hydrogels with very high molecular masses. This delays the degradation of the polymer.

The group from Šoltés *et al.* synthesized hydrogels for nonsurgical, viscosupplementatious applications [151]. Their patented system is the injection of a cocktail of two HyA derivates, namely, *n*-acetylurea-HyA and β-cyclodextrin-HyA, which spontaneously associate to hydrogels. To ensure that the hydrogel is not formed before the injection, a drug molecule is added which blocks the association process until it is degraded in the body. A new synthetic route to these HyA derivates was proposed by Charlot *et al.* [152]. Other hydrogels for viscoaugmentation applications were described by Shu *et al.*, who synthesized thiolated HyA derivatives and formed hydrogels through disulfide crosslinking or by coupling to α,β-unsaturated esters and amides of polyethylene crosslinkers [153]. The polymerization time could be adjusted from 10 min up to several days, depending on the chemical structure of the crosslinker.

Pulpitt *et al.* and Jia *et al.* used another crosslinking strategy based on hydrazide- and aldehyde-modified HyA [154, 155]. The hydrazide is generated through coupling of adipic dihydrazide to the carboxylic groups of HyA. The aldehyde-modified HyA can be obtained by oxidation of the diol moiety with sodium periodate. These two functional groups react spontaneously to hydrogels via hydrazone formation. Another hydrogel formation mechanism is described by Kurisawa *et al.* who synthesized an injectable HyA–tyramine conjugates which polymerized via enzyme-induced oxidative coupling [156].

HyA can be used as drug carrier to improve the solubility of pharmaceuticals or to decrease their toxicity. A review from Bettolo *et al.* describes different HyA–paclitaxel bioconjugates, which overcome the initial mentioned problems [157]. Paclitaxel is a well-known antitumor agent used for the treatment of breast and ovarian cancer. A controlled release in the tumor region can be assumed due to the overexpression of the HyA CD 44 receptor in various cancer cell lines. Approaches toward HyA as carrier substrate for carboranes in boron neutron capture therapy have been made by Di Meo *et al.* [158]. This therapy includes the delivery of ^{10}B to the tumor tissue and irradiation thereof with small doses of thermal/epithermal neutrons. This leads to ablation of the malignant cells.

There are numerous applications and chemical modification strategies to use HyA in the field of drug delivery: (i) Motokawa *et al.* developed a strategy of sustained release of erythropoietin through noncovalent encapsulation in HyA hydrogels for anemia treatment synthesized with the aldehyde/hydrazine method [159]. (ii) Kinetics of the drug release of esterified HyA–steroid conjugates for the treatment of inflammatory joint diseases was studied with NMR [160]. (iii) HyA and polyglutamate block polymers were synthesized using "click chemistry" [161].

Nanovesicles were prepared thereof and cytotoxic agents such as doxorubicin were internalized for controlled drug release. (iv) Sorbi *et al*. introduced the coupling of methotrexate to the primary alcohol of HyA for the therapy of autoimmune diseases such as rheumatoid arthritis [162].

7.11 Pullulan

Pullulan is a water soluble, neutral polysaccharide consisting of maltotriose monomeric units interconnected by α-(1→4) glycosidic bonds, whereas maltrotriose sequences are combined to yield a polymeric chain by α-(1→6) glycosidic linkages. The structural formula corresponds to [α-D-Glc$_p$-(1→4)-α-D-Glc$_p$-(1→4)-α-D-Glc$_p$(1→6)]$_n$. The assembled polysaccharide strain may display some minor structural abnormalities like maltotetraose; however, chemical properties are not affected. The regular alteration of the glycosidic bonds results in two distinctive properties: structural flexibility and enhanced solubility. The first description of pullulan has been published by Wallenfels *et al*. in the 1960s, based on the analyzed fermentation medium of *Aureobasidium pullulans* [163] (Scheme 7.11).

Because of the coexistence of α-(1→4)- and α-(1→6)-bonds in the chain, the overall structure is an intermediate between amylose and dextran. Native water-soluble pullulan is produced extracellularly by several strains such as *A. pullulans*, *Pullularia pullulans*, or *Dematium pullulans*. However, the bacterial cultures generate two different exopolysaccharides. Besides pullulan, a water-insoluble jelly-like β-(1→3)-glucan is also produced [164]. The detailed mechanism of the biosynthesis is not known yet, accordingly there is no explanation of the β-glucan formation. Some indications adumbrate the dependency on the individual genetic type of *A. pullulans* [165]. Local peculiarities of the biosynthesis with various *A. pullulans* strains have been investigated by Kondratyeva *et al* [166]. Pullulan can be synthesized from sucrose by cell-free enzymes of *A. pullulans* when both ATP and UDPG are added to a reaction mixture. In the case of glucose, mannose, galactose, fructose, or other carbon sources, the pathway is not clear [167]. The average molecular

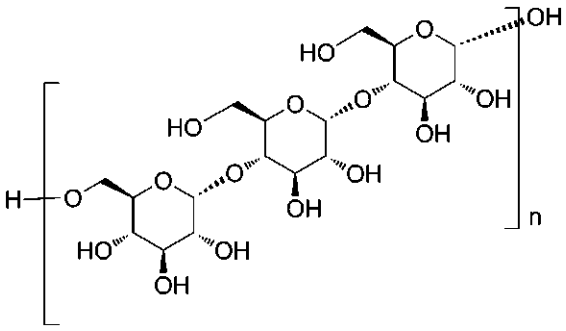

Scheme 7.11 Chemical structure of pullulan.

weight of pullulan varies in very broad ranges, from hundreds to thousands of kilodaltons, depending on the culture strain, pH, cultivation techniques, and substrates used [168]. As a subsumption of characteristics, pullulan is water soluble, nonhygroscopic in nature, moldable and spinnable, nontoxic, edible, and biodegradable. Due to these attributes, it is a good adhesive and binder and has capacity to form fibers, compression moldings, and strong oxygen-impermeable films. An actual survey about patents, new inventions related to production, cosmetical and pharmaceutical applications, as well as chemical derivatizations like esterification, etherification, hydrogenation, and carboxylation has been published by Singh *et al*. [169].

Pullulanase (pullulan-6-glucanohydrolase), which is a debranching enzyme, belongs to the family of glycosyl hydrolases. It is widely distributed among animals, plants, fungi, and bacteria and has the ability to hydrolyze α-glucosidic linkages. Complete hydrolysis of pullulan by both enzymes (1–6)-α-D- and (1–4)-α-D-pullulanase leads to isopanose as the main product. In some cases, partial hydrolysis yields isomaltose, maltose, or panose. The precise enzymatic mechanism of degradation and the resulting final product differs in each case [170] Thermal decomposition of the polymer chain occurs at temperatures about 250–280 °C.

Analogous to the broad family of polysaccharides based on glucose, chemical modifications can merely be done at one of the hydroxyl groups in the monomeric unit. As a result of the 1→4 linkages in the maltotriose units, the primary hydroxyl functions at the C-6 remain free. This leads to a higher reactivity of the C-6 alcohol compared to the C-2, C-3, and or C-4 position. Suitable modifications to carbonation, succinoylation, or carbamylation occur at the C-6 position. Nevertheless, the synthesis of carbomethylpullulan (CMP) by carboxymethylation proceeds predominantly at the C-2 position, similar to dextran. In order to establish a homogeneous sulfatation of pullulan, the reactivity of the different polysaccharide carbon atoms has been determined by Mähner *et al* [171]. They revealed the reactivity in the order C-6 > C-3 > C-2 > C-4. This result has been confirmed by Alban *et al*. who identified that the sulphatation occurs from C-6 to C-4, irrespective of the molecular weight, the production and the degree of substitution [172]. Furthermore, alkyl building blocks like chloroalkyl chlorides, chloroacetyl chlorides, or cholesteryl groups were attached to the polymeric chain. They were used to crosslink chains or form hydrogels [173]. Remarkable are syntheses with perfluoroalkyl carboxylic acids or amines in order to get alkylfluoronated compounds [174]. Consequently, pullulan and its derivatives have broad potential for food, pharmaceutical, and industrial applications.

In order to establish medical applications, the biological activity of pullulan was determined. The analyses have shown that pullulan has no mutagenic, carcinogenic, or toxicological activities, but exhibits a great affinity toward the liver and is effectively endocytosed by the parenchymal liver cells. This affinity toward liver cells qualifies pullulan as a drug delivery polymer for hepatitis therapy [175]. According to the great analogy to dextran, pullulan was also attempted for use as a blood-plasma substitute. In contrast to the assumptions, pullulan possess a short half-life in the blood, considered to the great affinity toward liver. CMP is

pronounced as an auspicious drug carrier. The introduced carboxylic acid moiety induces a negative charge to the polysaccharide which results in a prolonged retention of the macromolecule within the organism [176]. CMP was found to be selectively absorbed by the spleen and lymph nodes. This fact allows the development of a new application spectrum of pullulan as immunodepressant conjugate [177]. Up to now, several CMP silalyl Lewis^X conjugates are applied to target inflammation sites, or CMP-doxorubicin derivatives were synthesized and evaluated for their antitumor activity. Analogous to the well-known anticoagulant heparin or dextran-sulfate, pullulan-sulfate has been engineered, where the gained activity is almost comparable with that of heparin. Through combination of highly hydrophilic polysaccharide chains with native or synthetic hydrophobic moieties, new promising novel biologically active compounds can be created. In the form of nanoparticles, they can find application as drug-delivery system and for the thermal and colloidal stabilization of proteins. These compact nanoparticles are formed by intermolecular aggregation of hydrophobized polysaccharides, whereas the strength of the self-association can be regulated by the length of the hydrophobic moiety [174]. The already mentioned notable fluoro derivatives are utilized as fluorosurfactant or oxygen carrier. Fluorosurfactants are necessary for targeting delivery of drugs or as contrasting agents. The latter unique ability to dissolve oxygen 20 times higher than that of blood plasma enables the development of injectable forms of perfluorocarbon-based oxygen carriers, which have no toxic or reactivity-related side effects and can be removed easily form the organism via excretion [178].

7.12 Scleroglucan

Scleroglucan is a branched homopolysaccharide, which only consists of D-glucose moieties. The polymer has a main chain of β-(1→3)-linked D-glucopyranose units. Every third glucose is substituted at position 6 with a single β-D-glucopyranose (Scheme 7.12).

The polymer is produced extracellularly by the heterotrophic filamentous fungi of the genus *Sclerotium*, for example, *Sclerotium glucanicum*, *Sclerotium rolfsii*, and *Sclerotium delphinii*. For industrial fermentation processes, mainly *S. glucanicum* and *S. rolfsii* were used. In the plant pathogenic fungi *Sclerotium* sp., scleroglucan enables the attachment of the parasite to the plant surfaces and protects the fungi against desiccation. Under optimal fermentation conditions, a maximum yield of 8.5–10 g/L scleroglucan can be obtained using *S. glucanicum*. In contrast, high sucrose fermentation of *S. rolfsii* results in an isolated yield of up to 21 g/L. Depending on the strain and the fermentation conditions, the molecular weight of scleroglucan ranges between 1.3×10^5 and 6.0×10^6 g mol^{-1}. Schizophyllan, a polysaccharide isolated from *Schizophyllum* sp., has the same molecular composition as scleroglucan but is reported with a molecular weight of 6.12×10^6 g mol^{-1} [179].

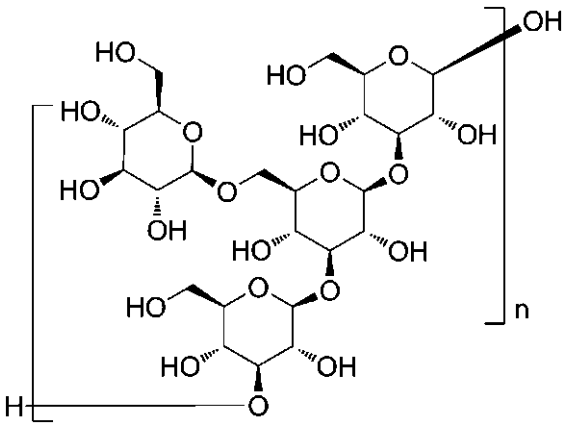

Scheme 7.12 Chemical structure of scleroglucan.

Scleroglucan readily dissolves in water and forms rigid, right-handed, triple-helical structure. The interstrand aggregation of the helices is disturbed by the side glucose groups, which protrude from the helix. The scleroglucan helix structure is thermostable, but instable at pH higher than 12.5 or toward organic solvents such as dimethyl sulfoxide. The helical structure of scleroglucan in solution is responsible for rheological properties. It forms viscous pseudoplastic solutions, which tolerate several salts, high temperature (10–90 °C), and broad pH range (pH 1 to 11) without major changes in the viscosity. Retaining more than 90% of its viscosity after 500 days at 90 °C in seawater, scleroglucan was the most stable compound among 140 other polymers tested for use in polymer flooding in oil reservoirs [179, 180].

Scleroglucan is compatible with many electrolytes such as sodium chloride (5%), sodium sulfate (5%), calcium chloride (20%), and disodium hydrogen phosphate (10%) without major changes in the rheological properties [179]. In contrast, a hydrogel gel can be obtained by addition of borax (0.1 mol borax for 1 mol repeating unit of scleroglucan) to the aqueous polymer solution. The final polymer concentration in the stable hydrogel is 0.7% (w/v) [181, 182]. Oxidation of the glucose side chain in scleroglucan using sodium periodate results in the formation of dialdehyde groups (scleraldehyde) and the production of formic acid. During the initial periodate oxidation, an increase in the storage modulus associated with the formation of gels can be observed. The mechanism of gellation can be explained by the formation of intermolecular hemiacetal linkages. These gels are to be physically stable, whereas aldehyde reduction (using sodium borohydride) or oxidation to carboxyl (using sodium chlorite) dissolved the gels [183]. The corresponding polymeric carboxylic acid after sodium chlorite oxidation is also known as sclerox and was studied in detail [184]. Scleraldehyde with a low degree of oxidation (10% and 20%), prepared by a controlled oxidation of scleroglucan, is reported to retain essentially a triple-stranded helical conformation, while the triple-stranded chains separate in single chains with increasing the degree of oxidation (40% and 100%).

The hydrogel prepared from scleraldehyde with a low degree of oxidation by crosslinking with diamines can be represented by a network composed of randomly oriented triple helices interlinked at the sites where the aldehyde groups are present [185].

The first industrial application of scleroglucan was in oil recovery, where it showed better pH and temperature stability than xanthan. In watered-out reservoirs, where seawater pressure is no longer sufficient to recover the oil, the addition of scleroglucan to improve the viscosity of the feed water can improve the process significantly. Additionally, scleroglucan lubricates the drill and controls the backpressures created during drilling [179]. In the field of pharmaceutics, numerous studies are published on applications of scleroglucan both in its native form and as derivatives. Hydrogels obtained by different crosslinking agents are suitable for a release modulation from various dosage forms. Sustained release and environment-controlled delivery systems that can be obtained from crosslinked scleroglucan represent a challenging field of applications [186]. There are numerous additional applications using the superb rheological properties and the high stability of scleroglucan ranging from food and cosmetics to paints and ceramic glazes. In most of these cases, scleroglucan is a competitor of xanthan [187].

7.13 Xanthan

Xanthan is a polysaccharide with a cellulose backbone of β-(1→4) linked D-glucose. Every second glucose is substituted at position 3 with a side chain consisting of β-D-mannose-(1→4)-β-D-glucuronic acid-(1→2)-α-D-mannose. The terminal mannose moiety is partially substituted with a pyruvate, coupled as an acetal at positions 4 and 6. The internal mannose usually bears an acetate group at position 6. The degree of pyruvate substitution varies between 30% and 40%, whereas 60–70% of the internal mannose units are acetylated. The molecular weight of xanthan is about 1,000,000 g mol^{-1} (Scheme 7.13).

Because of the glucuronic acid moieties and the partial pyruvate substituents in the side chain, xanthan is an ionic polysaccharide and its polyelectrolytic character in water was studied in detail [188].

The polymer is produced by the fermentation with the bacteria *Xanthomonas campestris* [189], *Xanthomonas phaseoli* [190], and *Xanthomonas jugIandis* [191] and other *Xanthomonas* species with an annual production of approximately 30,000 tons. The pyruvyl and acetyl content of xanthan isolates depends on the fermentation conditions and bacterial strain [192]. As shown for *X. campestris*, the production, composition, and viscosity of the xanthan synthesized by this strain are influenced by the fermentation time and nutrient exhaustion in batch culture and by the dilution rate in continuous culture. The specific rate of xanthan synthesis is maximal during exponential growth, although some xanthan is also formed during the stationary phase [189]. Under optimized conditions, a production of up to 22 g/L xanthan can be reached in a stirred tank fermentor [193]. As the product

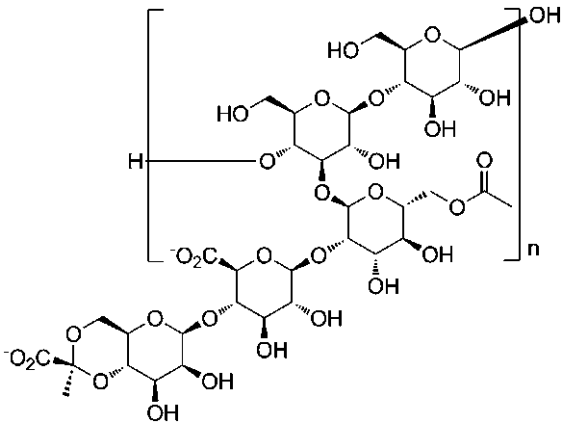

Scheme 7.13 Chemical structure of xanthan.

accumulates, the broth viscosity increases dramatically and the broth rheology presents serious problems to mixing, heat transfer, and oxygen input. This limiting factor of the process efficiency can be overcome by water-in-oil cultivation technologies, where the xanthan produced stays within the aqueous droplets dispersed in an immiscible organic phase (e.g., vegetable oil or *n*-hexadecane) and the effective viscosity of the overall system is kept low. Xanthan concentrations of more than 200 g/L culture medium can be reached by this approach [194].

Xanthan is known as a highly stable polysaccharide, which is not easily degraded by microorganisms. Still some microorganisms such as *Bacillus* sp. 13–4, *Paenibacillus alginolyticus* XL-1, *Cellulomonas* sp. LX, *Microbacterium* sp. XT11, and *Paenibacillus* sp. XD were reported to participate in depolymerization of xanthan [195]. The enzymatic basis of xanthan degradation was studied by Nankai *et al.* who analyzed the structures of xanthan depolymerization product by electrospray mass spectrometry and identified the enzymes involved in the process. In *Bacillus* sp., GL1 Xanthan is depolymerized to constituent monosaccharides by two extracellular and three intracellular enzymes. In the initial step, the terminal pyruvate-substituted mannose is cleaved by a xanthan lyase and the polymeric backbone is subsequently depolymerized by a β-D-glucanase (endoxanthanase) [196]. Recently, a novel endoxanthanase catalyzing the hydrolysis of the main chain of xanthan with an intact side chain was isolated from *Microbacterium* sp. strain XT11 and characterized. This enzyme may be used in the treatment of *Xanthomonas* infectious disease or for the biodegradation of xanthan injected into underground oil [197].

Xanthan is easily soluble in cold and hot water. The viscosity of the xanthan solution is nearly independent of temperatures up to 90 °C and of the pH value. Also higher salt concentrations have no big influence on the viscosity. The polymer has relatively good stability during sterilization and the solutions are very stable toward chemical, enzymatic, or bacterial degradation allowing a wide range of applications. Also xanthan can be crosslinked, gelled, and associated with other

biopolymers such as alginates, carrageenans, galactomannans, gelatin, glucomannans, or pectins.

The practical use of xanthan gum is mainly due to its ability to induce high viscosity at low polymer concentration in an aqueous environment. It also has a unique shear thinning behavior and is less prone to degradation compared with other polysaccharides. Major markets of this biopolymer exist in food, ceramic glazing, and petroleum drilling industries. In 1969, FDA allowed xanthan for the general use in foods. Typical food applications of xanthan gum are salad dressings, sauces, gravies, dairy products, desserts, low-calorie foods, and convenience foods in general. Xanthan gum is also used in cleaners, coatings, polishes, and agricultural flowables. Furthermore, it is used as an agent in many toothpastes and cosmetic preparations [198].

The main pharmaceutical application of xanthan is the usage as tablet excipient to modulate the rate of drug delivery and drug release [4]. In a recent study, crosslinked starch–xanthan hydrogels are synthesized and the new hydrogels has a good film forming ability. The equilibrium swelling ratio, swelling rate, gel mesh size, and drug permeability of the starch–xanthan hydrogels increase with increasing crosslinker and xanthan content. The mesh sizes of the hydrogels are 2.84–6.74 nm at pH 7.4 depending on the gel composition. This mesh size range is large enough to transport most drugs from small molecules to polypeptide and proteins. The hydrogel exhibits selective permeability depending on drug charges, allowing the design of controlled release formulations of ionizable drugs [199]. No crosslinker is necessary when polyionic hydrogels are formed through interaction of the polyanion xanthan with a polycation such as chitosan. This hydrogel is porous, has a fibrous structure, good hygroscopic qualities, and is capable of immobilizing bioactive substances such as drugs or enzymes. The channels present in the fibrillar gels have a pore size between 0.1 and 1 μm, whereas the fibrils have a diameter of 0.1 μm. The polyionic hydrogel has the advantage of creating an ionic microsystem which favors the stabilization of a protein polymer by interacting with the free acid and base functions. Thus, upon coimmobilization of protease and xylanase in the xanthan-based hydrogel, the protease acitivity is increased up to 85% [200].

7.14 Summary

Polysaccharides are ubiquitous naturally occurring renewable polymers, which can be isolated from various sources such as plants, animals, and microorganisms. In nature, polysaccharides were used for energy storage, as scaffold, as signaling, and shielding element. Polysaccharides exhibit an enormous structural diversity due to different monosaccharide composition, different linkage types and patterns, and a wide spectrum of molecular weights. As a direct consequence, their physical, chemical, and biological properties are well dispersed. The next level of complexity is introduced by chemical modifications such as chain decorations and crosslink-

ages. Therefore, polysaccharides have a wide range of potential applications ranging from tissue engineering and regenerative medicine over food additives to explosives, deflocculants in paper industry, and oil drilling muds.

Degradability or even biodegradability is hard to define in this context and in some cases even partial depolymerization is considered as degradation. Several polysaccharides are readily degradable in vertebrates such as HyA and chitin. Several tissue engineering applications were reported for this class of polymers, and fine-tuning the degradation kinetics is an important field of research. Other polymers such as gellan, xanthan alginate, and cellulose are mainly degraded by bacteria using the polymer as energy source. As one example, all organisms known to degrade cellulose efficiently produce a battery of highly diverse enzymes with different specificities, which act together in synergism. These polysaccharides were mainly used for technical or food applications due to their rheological and material properties or as degradable excipient in tablets pharmaceutical formulations. Belonging to the bacterial degradable polymers, alginate with its unique material properties and characteristics has also been increasingly considered as biomaterial for medical applications. CA gels have unique intrinsic properties and exhibit biocompatibility, mucoadhesion, porosity, and ease of manipulation. Hence, much attention has recently been focused on alginate-based materials for protein delivery, cell encapsulation, and tissue regeneration.

Acknowledgments

Financial support was provided by funding from the Deutsche Forschungsgemeinschaft (DFG, German Research Foundation) for the Cluster of Excellence REBIRTH (From Regenerative Biology to Reconstructive Therapy).

In Memoriam

Professor Severian Dumitriu was a highly esteemed scientist and teacher and a wonderful human being. His legacy will live on within the polymeric research community through his significant contributions (over 180 scientific papers and book chapters). He devoted his life to polymeric biomaterials field progress, promoting scientific excellence and training future generations of scientists. When he started on this chapter no one could ever have imagined that he could not finalize it. Professor Dumitriu's family is grateful to the co-authors and book editors for completion and final review of this chapter.

References

1 Rinaudo, M. (2008) *Polym. Int.*, **57**, 397–430.

2 Mano, J.F., Silva, G.A., Azevedo, H.S., Malafaya, P.B., Sousa, R.A., Silva, S.S.,

Boesel, L.F., Oliveira, J.M., Santos, T.C., Marques, A.P., Neves, N.M., and Reis, R.L. (2007) *J. R. Soc. Interface*, **4**, 999–1030.
3 Liu, Z., Jiao, Y., Wang, Y., Zhou, C., and Zhang, Z. (2008) *Adv. Drug Deliv. Rev.*, **60**, 1650–1662.
4 Coviello, T., Matricardi, P., Marianecci, C., and Alhaique, F. (2007) *J. Control. Release*, **119**, 5–24.
5 Remminghorst, U. and Rehm, B.H.A. (2006) *Biotechnol. Lett.*, **28**, 1701–1712.
6 De Vos, P., De Haan, B., and Van Schilfgaarde, R. (1997) *Biomaterials*, **18**, 273–278.
7 Haug, A., Larsen, B., and Smidsrød, O. (1967) *Acta Chem. Scand.*, **21**, 691–704.
8 Sutherland, I.W. (1995) *FEMS Microbiol. Rev.*, **16**, 323–347.
9 Gimmestad, M., Ertesvåg, H., Heggeset, T.M.B., Aarstad, O., Svanem, B.I.G., and Valla, S. (2009) *J. Bacteriol.*, **191**, 4845–4853.
10 Sikorski, P., Mo, F., Skjåk-Bræk, G., and Stokke, B.T. (2007) *Biomacromolecules*, **8**, 2098–2103.
11 Thom, D., Grant, G.T., Morris, E.R., and Rees, D.A. (1982) *Carbohydr. Res.*, **100**, 29–42.
12 Thu, B., Smidsrød, O., and Skjåk-Bræk, G. (1996) *Immobilized Cells; Basics and Applications*, Elsevier Science, Amsterdam.
13 Seale, R., Morris, E.R., and Rees, D.A. (1982) *Carbohydr. Res.*, **110**, 101–122.
14 Gomez, C.G., Rinaudo, M., and Villar, M.A. (2007) *Carbohydr. Polym.*, **67**, 296–304.
15 Soon-Shiong, P., Desai, N.P., Sandford, P.A., Heintz, R.A., and So-Jomihardjo, S. (1993) Crosslinkable polysaccharides, polycations and lipids useful for encapsulation and drug release, Patent WO 93/09176.
16 Jeon, O., Bouhadir, K.H., Mansour, J.M., and Alsberg, E. (2009) *Biomaterials*, **30**, 2724–2734.
17 Baroli, D. (2006) *J. Chem. Technol. Biotechnol.*, **81**, 491–499.
18 Augst, A.D., Kong, H.J., and Mooney, D.J. (2006) *Macromol. Biosci.*, **6**, 623–633.
19 Ossipov, D.A., Piskounova, S., and Hilborn, J. (2008) *Macromolecules*, **41**, 3971–3982.
20 Bouhadir, K.H., Alsberg, E., and Mooney, D.J. (2001) *Biomaterials*, **22**, 2625–2633.
21 Bouhadir, K.H., Kruger, G.M., Lee, K.Y., and Mooney, D.J. (2000) *J. Pharm. Sci.*, **89**, 910–919.
22 Rowley, J.A., Madlambayan, G., and Mooney, D.J. (1999) *Biomaterials*, **20**, 45–53.
23 Fonder, M.A., Lazarus, G.S., Cowan, D.A., Aronson-Cook, B., Kohli, A.R., and Mamelak, A.J. (2008) *J. Am. Acad. Dermatol.*, **58**, 185–206.
24 Terrill, P.J., Goh, R.C.W., and Bailey, M.J. (2007) *J. Wound Care*, **16**, 433–438.
25 Chiu, C.-T., Lee, J.-S., Chu, C.-S., Chang, Y.-P., and Wang, Y.-J. (2008) *J. Mater. Sci. Mater. Med.*, **19**, 2503–2513.
26 Poucke, S.V., Jorens, P.G., Peeters, R., Jacobs, W., de Beeck, B.O., Lambert, J., and Beaucourt, L. (2004) *Int. Wound J.*, **1**, 207–213.
27 Jude, E.B., Apelqvist, J., Spraul, M., Martini, J., and the Silver Dressing Study Group (2007) *Diabet. Med.*, **24**, 280–288.
28 Ahmad, Z., Pandey, R., Sharma, S., and Khuller, G.K. (2006) *Indian J. Chest. Dis. Allied Sci.*, **48**, 171–176.
29 Mazumder, M.A.J., Shen, F., Burke, N.A.D., Potter, M.A., and Stöver, H.D.H. (2008) *Biomacromolecules*, **9**, 2292–2300.
30 Paul, A., Ge, Y., Prakash, S., and Shum-Tim, D. (2009) *Regenerative Med.*, **4**, 733–745.
31 Dang, T.T., Xu Q., Bratlie K.M., O'Sullivan, E.S., Chen X.Y., Langer, R., and Anderson, D.G. (2009) *Biomaterials*, **30**, 6896–6902.
32 Becker T.A., Preul M.C., Bichard W.D., Kipke D.R., and McDouqall C.G. (2007) *Neurosurgery*, **60**, 1119–1127.
33 Kedem, A., Perets, A., Gamlieli-Bonshtein, I., Dvir-Ginzberg, M., Mizrahi, S., and Cohen, S. (2005) *Tissue Eng.*, **11**, 715–722.
34 Bretagne, J.F., Richard-Molard, B., Honnorat, C., Caekaert, A., and Barthélemy, P. (2006) *Presse Med.*, **35**, 23–31.
35 Cresi, F., Savino, F., Marinaccio, C., and Silvestro, L. (2006) *Arch. Dis. Child.*, **91**, 93.

36 Dettmar, P.W., Sykes, J., Little, S.L., and Bryan, J. (2006) *Int. J. Clin. Pract.*, **60**, 275–283.

37 Tang, M., Dettmar, P., and Batchelor, H. (2005) *Int. J. Pharm.*, **292**, 169–177.

38 Hashimoto, T., Suzuki, Y., Suzuki, K., Nakashima, T., Tanihara, M., and Ide, C. (2005) *J. Mater. Sci. Mater. Med.*, **16**, 503–509.

39 De Ruiter, G.A., and Rudolph, B. (1997) *Trends Food Sci. Technol.*, **8**, 389–395.

40 Collén, P.N., Lemoine, M., Daniellou, R., Guégan, J.-P., Paoletti, S., and Helbert, W. (2009) *Biomacromolecules*, **10**, 1757–1767.

41 Michel, G., Chantalat, L., Fanchon, E., Henrissat, B., Kloareg, B., and Dideberg, O. (2001) *J. Biol. Chem.*, **276**, 40202–40209.

42 Ohta, Y. and Hatada, Y. (2006) *J. Biochem.*, **140**, 475–481.

43 Guibet, M., Kervarec, N., Génicot, S., Chevolot, Y., and Helbert, W. (2006) *Carbohydr. Res.*, **341**, 1859–1869.

44 Černíková, M., Buňka, F., Pavlínek, V., Březina, P., Hrabě, J., and Valášek, P. (2008) *Food Hydrocolloids*, **22**, 1054–1061.

45 Tapia, C., Escobar, Z., Costa, E., Sapag-Hagar, J., Valenzuela, F., Basualto, C., Gai, M.N., and Yazdani-Pedram, M. (2004) *Eur. J. Pharm. Biopharm.*, **57**, 65–75.

46 Piyakulawat, P., Praphairaksit, N., Chantarasiri, N., and Muangsin, N. (2007) *AAPS PharmSciTech*, **8**, 120–130.

47 Keppeler, S., Ellis, A., and Jacquier, J.C. (2009) *Carbohydr. Polym.*, **78**, 973–977.

48 (a) Payen, A. and Hebd, C.R. (1838) *Seances Acad. Sci.*, **7**, 1052; (b) Payen, A. and Hebd, C.R. (1838) *Seances Acad. Sci.*, **7**, 1125.

49 (a) Finaev, D. (2007) *Biol. Plant.*, **51**, 407–413; (b) Bessueille, L. and Bulone, V. (2008) *Plant Biotechnol.*, **25**, 315–322.

50 Kobayashi, S., Sakamoto, J., and Kimura, S. (2001) *Prog. Polym. Sci.*, **26**, 1525–1560.

51 Klemm, D., Heublein, B., Fink, H.P., and Bohn, A. (2005) *Angew. Chem. Int. Ed.*, **44**, 3358–3393.

52 Bochek, A.M. (2003) *Russ. J. Appl. Chem.*, **76**, 1711–1719.

53 (a) Potthast, A., Rosenau, T., Buchner, R., Röder, T., Ebner, G., Bruglachner, H., Sixta, H., and Kosma, P. (2002) *Cellulose*, **9**, 41–53; (b) Ciacco, G.T., Liebert, T.F., Frollini, E., and Heinze, T.J. (2003) *Cellulose*, **10**, 125–132; (c) Saalwächter, K., Buchard, W., Klüfers, P., Kettenbach, G., Mayer, P., Klemm, D., and Dugarmaa, S. (2000) *Macromolecules*, **33**, 4094–4107.

54 Bajerová, M., Krejčová, K., Rabišková, M., Gajdziok, J., and Masteiková, R. (2009) *Adv. Polym. Tech.*, **28**, 199–208.

55 El Seoud, O.A. and Heinze, T. (2005) *Adv. Polym. Sci.*, **186**, 103–149.

56 Edgar, K.J., Buchanan, C.M., Debenham, J.S., Rundquist, P.A., Seiler, B.D., Shelton, M.C., and Tindall, D. (2001) *Prog. Polym. Sci.*, **26**, 1605–1688.

57 (a) Becher, J., Liebegott, H., Berlin, P., and Klemm, D. (2004) *Cellulose*, **11**, 119–126; (b) Tiller, J., Klemm, D., and Berlin, P. (2001) *Des. Monomers Polym.*, **4**, 315–328.

58 Kamel, S., Ali, N., Jahangir, K., Shah, S.M., and El-Gendy, A.A. (2008) *Express Polym. Lett.*, **2**, 758–778.

59 Sannino, A., Madaghiele, M., Conversano, F., Mele, G., Maffezzoli, A., Netti, P.A., Ambrosio, L., and Nicolais, L. (2004) *Biomacromolecules*, **5**, 92–96.

60 Rokhade, A.P., Agnihotri, S.A., Patil, S.A., Mallikarjuna, N.N., Kulkarni, P.V., and Aminabhavi, T.M. (2006) *Carbohydr. Polym.*, **65**, 243–252.

61 Brown, A.J. (1886) *J. Chem. Soc. Trans.*, **49**, 432–439.

62 Chawla, P.R., Bajaj, I.B., Survase, S.A., and Singhal, R.S. (2009) *Food Technol. Biotechnol.*, **47**, 107–124.

63 Shoda, M. and Sugano, M. (2005) *Biotechnol. Bioprocess Eng.*, **10**, 1–8.

64 Ross, P., Mayer, R., and Benziman, R. (1991) *Microbiol. Rev.*, **55**, 35–58.

65 Iguchi, M., Yamanaka, S., and Budhiono, A. (2000) *J. Mater. Sci.*, **35**, 261–270.

66 Czaja, W.K., Young, D.J., Kawecki, M., and Brown, R.M. Jr. (2007) *Biomacromolecules*, **8**, 1–12.

67 Helenius, G., Bäckdahl, H., Bodin, A., Nannmark, U., Gatenholm, P., and Risberg, B. (2006) *J. Biomed. Mater. Res.*, **76A**, 431–438.

68 Czaja, W., Krystynowicz, A., Bielecki, S., and Brown, R.M. Jr. (2006) *Biomaterials*, **27**, 145–151.

69 Legeza, V.I., Galenko-Yaroshevskii, V.P., Zinov'ev, E.V., Paramonov, B.A., Kreichman, G.S., Turkovskii, I.I., Gumenyuk, E.S., Karnovich, A.G., and Khripunov, A.K. (2004) *Bull. Exp. Biol. Med.*, **138**, 311–315.

70 Yasuda, K., Gong, J.P., Katsuyama, Y., Nakayama, A., Tanabe, Y., Kondo, E., Ueno, M., and Osada, Y. (2005) *Biomaterials*, **26**, 4468–4475.

71 Charpentier, P.A., Maguire, A., and Wan, W. (2006) *Appl. Surf. Sci.*, **252**, 6360–6367.

72 Loures, B.R. (2004) Endoprosthesis process to obtain and methods used, Patent WO 2004/0455448 AI.

73 Novaes, A.B. Jr., Novaes, A.B., Grisi, M.F.M., Soares, U.N., and Gaberra, F. (1993) *Braz. Dent. J.*, **4**, 65–71.

74 de Macedo, N.L., da Silva Matuda, F., de Macedo, L.G.S., Monteiro, A.S.F., Valera, M.C., and Carvalho, Y.R. (2004) *Braz. Dent. Oral Sci.*, **3**, 395–400.

75 (a) Watanabe, K., Eto, Y., Takano, S., Nakamori, S., Shibai, H., and Yamanaka, S. (1993) *Cytotechnology*, **13** 107–114; (b) Märtson, M., Viljanto, J., Laippala, P., and Saukko, P. (1998) *Eur. Surg. Res.*, **30**, 419–425.

76 (a) Kumar, M.N.V. (2008) *React. Funct. Polym.*, **46**, 1–27; (b) Pillai, C.K.S., Paul, W., and Sharma, C.P. (2009) *Prog. Polym. Sci.*, **34**, 641–678.

77 Chang, K.L.B., Tsai, G., Lee, J., and Fu, W.-R. (1997) *Carbohydr. Res.*, **303**, 327–332.

78 Sannan, T., Kurita, K., and Iwakura, Y. (1976) *Makromol. Chem.*, **177**, 3589–3600.

79 Tsigos, I., Martinou, A., Kafetzopoulos, D., and Bouriotis, V. (2000) *Trends Biotechnol.*, **18**, 305–312.

80 Berger, L.R. and Weiser, R.S. (1957) *Biochim. Biophvs. Acta*, **26**, 517–521.

81 Amano, K.L. and Lto, E. (1978) *Eur. J. Biochem.*, **85**, 97–104.

82 Shigemasa, Y., Saito, K., Sashiwa, H., and Saimoto, H. (1994) *Int. J. Biol. Macromol.*, **16**, 43–49.

83 Hu, X., Du, Y., Tang, Y., Wang, Q., Feng, T., Yang, J., and Kennedy, J.F. (2007) *Carbohydr. Polym.*, **70**, 451–458.

84 Austin, P.R., Brine, C.J., Castle, J.E., and Zikakis, J.P. (1981) *Science*, **212**, 749–753.

85 Austin, P.R. (1988) *Methods Enzymol.*, **161**, 403–407.

86 Tamura, H. (2006) *Polym. Prep. Jpn.*, **55**, 1862.

87 Tamura, H., Nagahama, H., and Tokura, S. (2006) *Cellulose*, **13**, 357–364.

88 Somorin, O., Nishi, N., Tokura, S., and Noguchi, J. (1979) *Polym. J.*, **11**, 391–396.

89 Tokura, S., Nishi, N., Somorin, O., and Noguchi, J. (1980) *Polym. J.*, **12**, 695–700.

90 Kaifu, K., Nishi, N., Komai, T., Tokura, S., and Somorin, O. (1981) *Polym. J.*, **11**, 241–245.

91 Szosland, L. and East, C.C. (1995) *J. Appl. Polym. Sci.*, **58**, 2459–2466.

92 Urbanczyk, G., Lipp-Symonowicz, B., Szosland, I., Jeziorny, A., Urbaniak-Domagala, W., Dorau, K., Wrzosek, H., Sztajnowski, S., Kowalska, S., and Sztajnert, E. (1997) *J. Appl. Polym. Sci.*, **65**, 807–819.

93 Muzzarelli, R.A.A. (2009) *Carbohydr. Polymer*, **76**, 167–182.

94 Naessens, M., Cerdobbel, A., Soetaert, W., and Vandamme, E.J. (2005) *J. Chem. Technol. Biotechnol.*, **80**, 845–860.

95 Robyt, J.F. (1985) *Encyclopaedia of Polymer Science*, vol. 4 (ed. J.I. Kroschwitz), John Wiley & Sons, Inc., New York, pp. 753–767.

96 Remaud-Simeon, M., Willemot, R.-M., Sarçabal, P., de Montalk, G.P., and Monsan, P. (2000) *J. Mol. Catal., B Enzym.*, **10**, 117–128.

97 Hehre, E.J. (1956) *J. Biol. Chem.*, **222**, 739–750.

98 Kakuchi, T., Kusuno, A., Miura, M., and Kaga, H. (2000) *Macromol. Rapid Commun.*, **21**, 1003–1006.

99 Naessens, M., Cerdobbel, A., Soetraet, W., and Vandamme, E.J. (2005) *J. Ind. Microbiol. Biotechnol.*, **32**, 323–334.

100 Khalikova, E., Susi, P., and Korpela, T. (2005) *Microbiol. Mol. Biol. Rev.*, **69**, 306–325.

101 Larsson, A.M., Andersson, R., Ståhlberg, J., Kenne, L., and Jones, T.A. (2003) *Structure*, **11**, 1111–1121.

102 Heinze, T., Liebert, T., Heublein, B., and Hornig, S. (2006) *Adv. Polym. Sci.*, **205**, 199–291.

103 Van Tomme, S.R., and Hennink, W.E. (2007) *Expert Rev. Med. Devices*, **4**, 147–164.

104 Kim, S.-H. and Chu, C.-C. (2000) *J. Biomater. Appl.*, **15**, 23–46.

105 Hudson, S.P., Langer, R., Fink, G.R., and Kohane, D.S. (2010) *Biomaterials*, **31**, 1444–1452.

106 De Belder, A.N. (1996) *Polysaccharides in Medicinal Applications* (ed. S. Dumitriu), Marcel Dekker, New York, pp. 505–523.

107 Leathers, T.D. (2002) *Biopolymers Vol. 5, Polysaccharides I: Polysaccharides from Prokaryotes* (eds E.J. Vandamme, S. De Baets, and A. Steinbüchel), Wiley-VCH Verlag GmbH, Weinheim, pp. 299–321.

108 Porath, J. and Flodin, P. (1987) *Chromatographia*, **23**, 365–369.

109 Debelder, A.N. (1993) *Industrial Gums: Polysaccharides and Their Derivatives*, 3rd edn (eds R.L. Whistler and J.N. BeMiller), Academic Press, New York, pp. 513–542.

110 Lobene, R.R. (1979) *J. Dent. Res.*, **58**, 2381–2388.

111 Tako, M., Teruya, T., Tamaki, Y., and Konishi, T. (2009) *Colloid. Polym. Sci.*, **287**, 1445–1454.

112 Nampoothiri, K.M., Singhania, R.R., Sabarinath, C., and Pandey, A. (2003) *Process Biochem.*, **38**, 1513–1519.

113 Cascone, M.G., Barbani, N., Cristallini, C., Giusti, P., Ciardelli, G., and Lazzeri, L. (2001) *J. Biomater. Sci. Polymer Edn.*, **12**, 267–281.

114 Chandrasekaran, R., Pulgjaner, L.C., Joyce, K.L., and Arnott, S. (1988) *Carbohydr. Res.*, **181**, 23–40.

115 Tako, M. and Tamaki, H. (2005) *Polym. J.*, **37**, 498–505.

116 Kennedy, L. and Sutherland, I.W. (1994) *Microbiology*, **140**, 3007–3013.

117 Jung, Y.-J., Park, C.S., Lee, H.G., and Cha, J. (2006) *J. Microbiol. Biotechnol.*, **16**, 1868–1873.

118 Hashimoto, W., Sato, N., Kimura, S., and Murata, K. (1998) *Arch. Biochem. Biophys.*, **354**, 31–39.

119 Derekova, A., Sjøholm, C., Mandeva, R., Michailova, L., and Kambourova, M. (2006) *Extremophiles*, **10**, 321–326.

120 Hamcerencu, M., Desbrieres, J., Khoukh, A., Popa, M., and Riess, G. (2008) *Carbohydr. Polym.*, **71**, 92–100.

121 Dentini, M., Desideri, P., Crescenzi, V., Yuguchi, Y., Urakawa, H., and Kajiwara, K. (2001) *Macromolecules*, **34**, 1449–1453.

122 Bajaj, I.B., Survase, S.A., Saudagar, P.S., and Singhal, R.S. (2007) *Food Technol. Biotechnol.*, **45**, 341–354.

123 Smith, A.M., Shelton, R.M., Perrie, Y., and Harris, J.J. (2007) *J. Biomater. Appl.*, **22**, 241–254.

124 McCleary, B.V., Clark, A.H., Dea, I.C.M., and Rees, D.A. (1985) *Carbohydr. Res.*, **139**, 237–260.

125 Wientjes, R.H.W., Duits, M.H.G., Jongschaap, R.J.J., and Mellema, J. (2000) *Macromolecules*, **33**, 9594–9605.

126 Cheng, Y. and Prud'homme, R.K. (2000) *Biomacromolecules*, **1**, 782–788.

127 McCleary, B.V. and Matheson, N.K. (1983) *Carbohydr. Res.*, **119**, 191–219.

128 McCleary, B.V. (1979) *Carbohydr. Res*, **71**, 205–230.

129 McCutchen, C.M., Duffaud, G.D., Leduc, P., Petersen, A.R.H., Tayal, A., Khan, S.A., and Kelly, R.M. (1996) *Biotechnol. Bioeng.*, **52**, 332–339.

130 Pal, S. (2009) *J. Appl. Polym. Sci.*, **111**, 2630–2636.

131 (a) Lapasin, R., De Lorenzi, L., Pricl, S., and Torriano, G. (1995) *Carbohydr. Polym.*, **28**, 195–202; (b) Cheng, Y., Brown, K.M., and Prud'homme, R.K. (2002) *Biomacromolecules*, **3**, 456–461.

132 Singh, V., Tiwari, A., Tripathi, D.N., and Sanghi, R. (2004) *Carbohydr. Polym.*, **58**, 1–6.

133 Nayak, B.R. and Singh, R.P. (2001) *Eur. Polym. J.*, **37**, 1655–1666.

134 Soppirnath, K.S. and Aminabhavi, T.M. (2002) *Eur. J. Pharm. Biopharm.*, **53**, 87–98.

135 Thakur, S., Chauhana, G.S., and Ahn, J.-H. (2009) *Carbohydr. Polym.*, **76**, 513–520.

136 Tiwari, A., Grailer, J.J., Pilla, S., Steeber, D.A., and Gong, S. (2009) *Acta Biomater.*, **5**, 3441–3452.

137 Meyer, K. and Palmer, J.W. (1934) *J. Biol. Chem.*, **107**, 629–634.

138 Balazs, E.A., Laurent, T.C., and Jeanloz, R.W. (1986) *Biochem. J.*, **235**, 903.

139 Lapčik, L. Jr. and Lapčik, L. (1998) *Chem. Rev.*, **98**, 2663–2684.

140 Hargittai, I. and Hargittai, M. (2008) *Struct. Chem.*, **19**, 697–717.

141 Weigel, P.H., Hascall, V.C., and Tammi, M. (1997) *J. Biol. Chem.*, **272**, 13997–14000.

142 Kogan, G., Šoltés, L., Stern, R., and Gemeiner, P. (2007) *Biotechnol. Lett.*, **29**, 17–25.

143 Kakehi, K., Kinoshita, M., and Yasueda, S. (2003) *J. Chromatogr. B*, **797**, 347–355.

144 Stern, R., Asari, A.A., and Sugahara, K.N. (2006) *Eur. J. Cell Biol.*, **85**, 699–715.

145 Stern, R. and Jedrzejas, M.J. (2006) *Chem. Rev.*, **106**, 818–839.

146 Meyer, K. and Rapport, M.M. (1952) *Adv. Enzymol.*, **13**, 199–236.

147 Volpi, N., Schiller, J., Stern, R., and Šoltés, L. (2009) *Curr. Med. Chem.*, **16**, 1718–1745.

148 Stern, R., Kogan, G., Jedrjas, M.J., and Šoltés, L. (2007) *Biotechnol. Adv.*, **25**, 537–557.

149 Lebel, L. (1991) *Adv. Drug Deliv. Rev.*, **7**, 221–235.

150 Balazs, E.A. (2004) *Chemistry and Biology of Hyaluronan*, Elsevier, Amsterdam.

151 (a) Šoltés, L., Mendichi, R., Kogan, G., and Mach, M. (2004) *Chem. Biodivers.*, **1**, 468–472; (b) Šoltés, L. and Mendichi, R. (2003) *Biomed. Chromatogr.*, **17**, 376–384.

152 Charlot, A., Heyraud, A., Guenot, P., Rinaudo, M., and Auzély-Velty, R. (2006) *Biomacromolecules*, **7**, 907–913.

153 (a) Shu, X.Z., Liu, Y., Palumbo, F.S., Luo, Y., and Prestwich, G.D. (2004) *Biomaterials*, **25**, 1339–1348; (b) Shu, X.Z., Liu, Y., Roberts, M.C., and Prestwich, G.D. (2002) *Biomacromolecules*, **3**, 1304–1311; (c) Shu, X.Z., Liu, Y., Palumbo, F., and Prestwich, G.D. (2003) *Biomaterials*, **24**, 3825–3834; (d) Shu, X.Z., Ahmad, S., Liu, Y., and Prestwich, G.D. (2006) *J. Biomed. Mater. Res. A*, **79A**, 902–912.

154 Bulpitt, P. and Aeschlimann, D. (1999) *J. Biomed. Mater. Res.*, **47**, 152–169.

155 Jia, X., Colombo, G., Padera, R., Langer, R., and Kohane, D.S. (2004) *Biomaterials*, **25**, 4797–4804.

156 Kurisawa, M., Chung, J.E., Yang, Y.Y., Gao, S.J., and Uyama, H. (2005) *Chem. Commun.*, **34**, 4312–4314.

157 Leonelli, F., Bella, A.L., Migneco, L.M., and Bettolo, R.M. (2008) *Molecules*, **13**, 360–378.

158 Di Meo, C., Panza, L., Capitani, D., Mannina, L., Banzato, A., Rondina, M., Renier, D., Rosato, A., and Crescenzi, V. (2007) *Biomacromolecules*, **8**, 552–559.

159 Motokawa, K., Hahn, S.K., Nakamura, T., Miyamoto, H., and Shimoboji, T. (2006) *J. Biomed. Mater. Res.*, **78A**, 459–465.

160 Taglienti, A., Sequi, P., and Valentini, M. (2009) *Carbohydr. Res.*, **344**, 245–249.

161 Upadhyay, K.K., Le Meins, J.-F., Misra, A., Voisin, P., Bouchaud, V., Ibarboure, E., Schatz, C., and Lecommandoux, S. (2009) *Biomacromolecules*, **10**, 2802–2808.

162 Sorbi, C., Bergamin, M., Bosi, S., Dinon, F., Aroulmoji, V., Khan, R., Murano, E., and Norbeo, S. (2009) *Carbohydr. Res.*, **344**, 91–97.

163 Bender, H., Lehmann, J., and Wallenfels, K. (1959) *Biochim. Biophys. Acta*, **36**, 310–317.

164 Kataoka-Shirasugi, N., Ikuta, J., Kuroshima, A., and Misaki, A. (1994) *Biosci. Biotech. Biochem.*, **58**, 2145–2151.

165 Simon, L., Caye-Vaugien, C., and Bouchonneau, M. (1993) *J. Gen. Microbiol.*, **139**, 979–985.

166 Kondratyeva, T.F. (1981) *Uspechi Microbiology*, **16**, 175–192.

167 Hayashi, S., Hayashi, T., Takasaki, Y., and Imada, K. (1994) *J. Ind. Microbiol.*, **13**, 5–9.

168 Shingel, K.I. (2004) *Carbohydr. Res.*, **339**, 447–460.

169 Singh, R.S., Saini, G.K., and Kennedy, J.F. (2008) *Carbohydr. Polym.*, **73**, 515–531.

170 Singh, R.S., Saini, G.K., and Kennedy, J.F. (2010) *Carbohydr. Polym.*, **80**, 401–407.

171 Mähner, C., Lechner, M.D., and Nordmeier, E. (2001) *Carbohydr. Res.*, **331**, 203–208.

172 Alban, S., Schauerte, A., and Franz, G. (2002) *Carbohydr. Polym.*, **47**, 267–276.

173 Mocanu, G., Mihai, D., Dulong, V., Picton, L., Lecerf, D. (2011) *Carbohyd. Polym.*, **84**, 276–281.

174 Glinel, K., Huguet, J., and Muller, G. (1999) *Polymer*, **40**, 7071–7081.

175 Tabata, Y., Matsui, Y., Uno, K., Sokawa, Y., and Ikada, Y. (1999) *J. Interferon Cytokine Res.*, **19**, 287–292.

176 Yamaoka, T., Tabata, Y., and Ikada, Y. (1993) *Drug Deliv.*, **1**, 75–82.

177 Masuda, K., Sakagami, M., Horie, K., Nogusa, H., Hamana, H., and Hirano, K. (2001) *Pharm. Res.*, **18**, 217–223.

178 Riess, J.G. (1998) *Blood Substitutes: Methods, Products and Clinical Trials* (ed. T.M.S. Chang), Karger Landes Systems, Basel, pp. 101–126.

179 Survase, S.A., Saudagar, P.S., Bajaj, I.B., and Singhal, R.S. (2007) *Food Technol. Biotechnol.*, **45**, 107–118.

180 Brigand, G. (1993) Scleroglucan, in *Industrial Gums* (eds. R.L. Whistler and J.N. BeMiller), Academic Press, New York, USA, pp. 461–472.

181 Coviello, T., Grassi, M., Lapasin, R., Marino, A., and Alhaique, F. (2003) *Biomaterials*, **24**, 2789–2798.

182 Grassi, M., Lapasin, R., Coviello, T., Matricardi, P., Di Meo, C., and Alhaique, F. (2009) *Carbohydr. Polym.*, **78**, 377–383.

183 Christensen, B.E., Aasprong, E., and Stokke, B.T. (2001) *Carbohydr. Polym.*, **46**, 241–248.

184 Crescenzi, V., Gamini, A., Paradossi, G., and Torri, G. (1983) *Carbohydr. Polym.*, **3**, 273–286.

185 Maeda, H., Rambone, G., Coviello, T., Yuguchi, Y., Urakawa, H., Alhaique, F., and Kajiwara, K. (2001) *Int. J. Biol. Macromol.*, **28**, 351–358.

186 Coviello, T., Palleschi, A., Grassi, M., Matricardi, P., Bocchinfuso, G., and Alhaique, F. (2005) *Molecules*, **10**, 6–33.

187 Giavasis, I., Harvey, L.M., and McNeil, B. (2002) Scleroglucan, in *Biopolymers, Polysaccharides II*, vol. 6 (eds S. De Baets, E.J. Vandamme, and A. Steinbuchel), Wiley-VCH Verlag GmbH, Weinheim, p. 37.

188 Rinaudo, M. and Milas, M. (1982) *Carbohydr. Polym.*, **2**, 264–269.

189 Tait, M.I., Sutherland, I.W., and Clarke-Sturman, A.J. (1986) *J. Gen. Microbiol.*, **132**, 1483–1492.

190 Lilly, G.V., Wilson, A.H., and Leach, J.G. (1958) *Appl. Microbiol.*, **6**, 105–108.

191 Roseiro, J.C., Amaral Collaco, M.T., Esgalhado, M.E., and Emery, A.N. (1992) *Process Biochem.*, **27**, 167–175.

192 Rottava, I., Batesini, G., Silva, M.F., Lerin, L., de Oliveira, D., Padilha, F.F., Toniazzo, G., Mossi, A., Cansian, R.L., Luccio, M.D., and Treichel, H. (2009) *Carbohydr. Polym.*, **77**, 65–71.

193 Pons, A., Dussap, C.G., and Gros, J.B. (1990) *Bioprocess Eng.*, **5**, 107–114.

194 Kuttuva, S.G., Restrepo, A.S., and Ju, L.-K. (2004) *Appl. Microbiol. Biotechnol.*, **64**, 340–345.

195 Muchová, M., Růžička, J., Julinová, M., Doležalová, M., Houser, J., Koutný, M., and Bunková, L. (2009) *Water Sci. Tech.*, **60**, 965–973.

196 Nankai, H., Hashimoto, W., Miki, H., Kawai, S., and Murata, K. (1999) *Appl. Environ. Microbiol.*, **65**, 2520–2526.

197 Li, B., Guo, J., Chen, W., Chen, X., Chen, L., Liu, Z., and Li, X. (2009) *Appl. Biochem. Biotechnol.*, **159**, 24–32.

198 Katzbauer, B. (1998) *Polym. Degrad. Stab.*, **59**, 81–84.

199 Shalviri, A., Liu, Q., Abdekhodaie, M.J., and Wu, X.Y. (2009) *Carbohydr. Polym.*, **79**, 898–907.

200 Dumitriu, S. and Chornet, E. (1998) *Adv. Drug Deliv. Rev.*, **31**, 223–246.

8
Biodegradable Shape-Memory Polymers

Marc Behl, Jörg Zotzmann, Michael Schroeter, and Andreas Lendlein

8.1
Introduction

Shape-memory polymers (SMPs) can change their shape in a predefined way on demand when exposed to a suitable stimulus. They are able to change their shape as soon as the stimulus activates molecular switching moieties. At present, most investigated SMPs are thermosensitive, which means that the shape-memory effect (SME) is triggered by heat. They change their shape once the material softens as a result of exceeding a certain switching temperature (T_{switch}).

SMPs are mainly applied in the biomedical field in implants, surgical instruments, extracorporal devices, wound covers, as well as in controlled drug release devices. Prominent examples of applications in everyday life are heat shrinkable tubing and films [1, 2], which are used for insulating electronic wiring or for packing [3]. Here, mainly covalently crosslinked polyethylene is used. Shape-memory polyurethanes (SMPU) have been designed and synthesized [4], which are used in textiles as smart fabrics [5, 6]. Further rapidly developing application fields include self-deployable sun sails in spacecraft or space structure applications [7], intelligent medical devices [8], or implants for minimal invasive surgery (MIS) [9, 10]. In this chapter, (bio)degradable SMPs will be presented, and their synthesis and applications are introduced.

SMPs belong to the group of "actively moving" polymers [11]. Most SMPs investigated so far are dual-shape polymers. Recently, triple-shape and multi-shape materials having the capability of two or even more subsequent movements were developed [12–19]. Triple-shape materials can change their shape from a temporary shape A to a possible second temporary shape B and finally to a permanent shape C. The temporary shapes are obtained by mechanical deformation of the material's permanent shape C at a temperature $T > T_{switch}$ and subsequent fixation of these deformations at lower temperatures ($T < T_{switch}$). The synthesis and the processing of the material determine the permanent shape C. In SMPs reported so far, heat or light has been used as a stimulus to trigger the SME [4, 20–23]. Indirect actuation of the SME has also been realized by irradiation with

Handbook of Biodegradable Polymers: Synthesis, Characterization and Applications, First Edition. Edited by Andreas Lendlein, Adam Sisson.

infrared- [24] or UV-light [25], application of electric field [26, 27] or alternating magnetic fields [28–31], or lowering of T_{switch} below ambient temperature by plasticizers such as water [32]. The SME results from a combination of a suitable molecular architecture and a programming procedure. Therefore, intrinsic material properties such as thermal or mechanical properties can be adjusted to the needs of specific applications by small variations of molecular parameters, such as monomer ratio or main chain bonds. This approach of adjusting material properties enables the design of polymer systems. Furthermore, this approach enables the creation of multifunctional materials, which is an actual trend in polymer science. Multifunctionality is the targeted combination of material functions, which are not linked with each other [33]. Multifunctional SMP can be realized as multimaterial systems, for example, by the incorporation of particles in polymer matrices, in which each material contributes a certain function, or as one component systems by the integration of suitable functional groups or building blocks [34]. Promising approaches can be the combination of biofunctionality, hydrolytic degradability, and shape-memory functionality. Such multifunctional SMPs have a high potential for applications in the biomedical field such as MIS (see Section 8.4) [35]. In contrast to metal implants or nondegradable polymers, bioresorbable SMPs are advantageous as they do not require an additional surgery for implant removal. In addition, bulky implants created from bioresorbable SMPs and having a T_{switch} between room temperature and body temperature could be inserted to the application site through a small incision in a compressed or elongated temporary shape. As soon as the implant is placed in the body, it assumes body temperature and changes into its bulky application-relevant shape. Other promising biomedical applications include intelligent degradable suture materials, which tighten a wound with a predefined stress, stimuli-sensitive matrices for drug delivery applications, or active scaffolds for regenerative therapies.

The required bioresorbable SMPs can be realized by the introduction of hydrolyzable bonds as weak links in the polymer chain enabling the degradation of these polymers in the presence of water, which may be supported by enzymes. Figure 8.1 shows hydrolysable bonds used in degradable polymers, in order of their stability.

Biodegradable, synthetic polymers may have advantages compared to polymers from natural sources. They can be tailored to meet the specific requirements of certain applications, such as thermal and mechanical properties. In addition, the processability of synthetic polymers, for example, by extrusion or injection molding

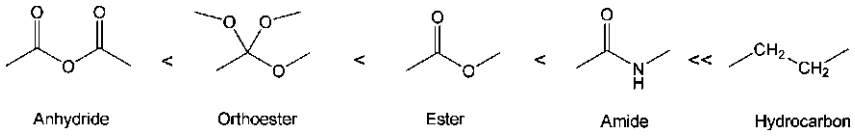

Figure 8.1 Relative stability of chemical bonds against hydrolysis occuring in common, synthetic polymers.

is much easier as they display in general a higher thermal stability as natural polymers. The tailoring of the polymer chain length of synthetic polymers enables polymers to form domains with a more defined domain size. When certain precautions are considered, a higher purity can be obtained, as a contamination with certain cell fragments can be avoided, which originate from the original source and can act as endotoxins. Consequently, polymers from natural sources require a high effort of purification, which potentially results in higher costs for such materials.

8.2
General Concept of SMPs

As the SME results from the combination of the polymer's molecular architecture/morphology and a specific programming procedure, it can be understood as a functionalization of the polymer. The shape-memory creation procedure (SMCP), which is also called programming, and the recovery of the original shape due to the SME are schematically shown in Figure 8.2.

Suitable polymeric materials that are capable of an SME provide a polymer network architecture consisting of netpoints, chain segments, and molecular switches, with the latter being sensitive to an external stimulus, which is heat in the case of the thermally induced SME.

The permanent shape of the SMP is determined by the netpoints, which are interconnected by the chain segments. The netpoints can be of chemical (covalent bonds) or physical (intermolecular interactions) nature. Covalent bonds can be formed by the application of a suitable crosslinking chemistry, while netpoints provided by intermolecular interactions require a morphology consisting of at least two segregated domains, for example, a crystalline and an amorphous phase. In such multiphase polymers, the polymer chain segments form domains. The domains that are related to the highest thermal transition temperature (T_{perm}) are called hard domains and are acting as physical netpoints.

In the course of SMCP when the temporary shape is created, a deformation is applied to the polymer sample. This deformation requires a sufficient elastic

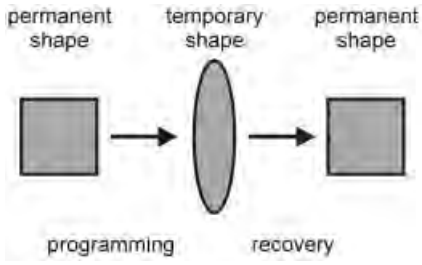

Figure 8.2 Schematic representation of the shape-memory effect. Taken from [4]. Copyright Wiley-VCH Verlag GmbH & Co. KGaA. Reproduced with permission.

deformability of the polymer network and can be reached by the chain segments, which must be capable to enable a certain orientation. The extent of the deformability increases with growing length and flexibility of these chain segments. In the polymer networks before applying the deformation, the majority of the polymer chain segments display a random coil conformation, which is the entropically favored orientation. The stimuli-triggered recoiling of the polymer chain segments, which is entropically driven, enables the recovery of the permanent shape.

The reversible fixation of the temporary shape is achieved by stimuli-sensitive switches that form additional reversible crosslinks, which can be established and cleaved on demand, and prevent in this way the recoiling of the polymer chain segments. Similarly to the permanent netpoints, these additional crosslinks can be established by the formation of chemical (covalent) reversible bonds, by the intermolecular interactions of side groups, or by the solidification of domains formed by these polymer chain segments when being cooled below their correlated thermal transition temperatures T_{trans}. Therefore, these polymer chain segments are also named switching segments; the associated domains are called switching domains. Such thermosensitive SMP can be classified according to the thermal transitions related to the solidification of the polymer chain segments. T_{trans} can be a glass transition temperature (T_g), a melting transition temperature (T_m), or a liquid crystalline transition. In all cases, heating of the SMP above the thermal transition causes a regain of flexibility of the vitrified or crystallized switching domains so that the elastic state is reached again. In thermoplastic SMP, only the domains associated to the polymer chain segments with the second highest T_{trans} are acting as switching domains.

Figure 8.3 displays a schematic representation of the molecular mechanism of the thermally induced SME, a thermoplastic SMP with $T_{trans} = T_m$, and covalent polymer networks with $T_{trans} = T_m$ (Figure 8.3b) or $T_{trans} = T_g$ (Figure 8.3c).

The SME can be quantified in cyclic, stimuli-specific tests under strain or stress control. Many degradable SMPs are triggered by heat as stimulus; consequently, the SME is determined in cyclic, thermomechanical tests. In these tests, the strain fixity rate (R_f), the strain recovery rate (R_r), and the switching temperature (T_{switch}) are determined. A single cycle includes the SMCP (programming) and the recovery of its permanent shape. The strain-controlled test consists of four steps: (1) heating of the sample to a temperature T_{high} above T_{trans} and deformation of the sample to a certain extension (ε_m) at a defined strain rate for a fixed period of time, (2) cooling to a temperature T_{low} with a certain cooling rate (β_c) while ε_m is kept constant, (3) unloading of the sample to $\sigma = 0$ MPa T_{low}, (4) heating of the test specimen to T_{high} while keeping the strain constant, and (5) start of the next cycle by going back to (1). In this test, the strain applied to the sample is controlled while the developing stress is recorded. In stress-controlled cyclic tests, steps (1) and (2) are adapted by keeping the stress σ constant at a maximum stress σ_m instead of keeping the sample at ε_m. The recovery step (4) is carried out by keeping $\sigma = 0$ MPa (Figure 8.4). In this test protocol, the deformation of the sample is monitored while the stress is controlled. T_{high} and T_{low} are adjusted to $T_{trans} \pm (20–30)$

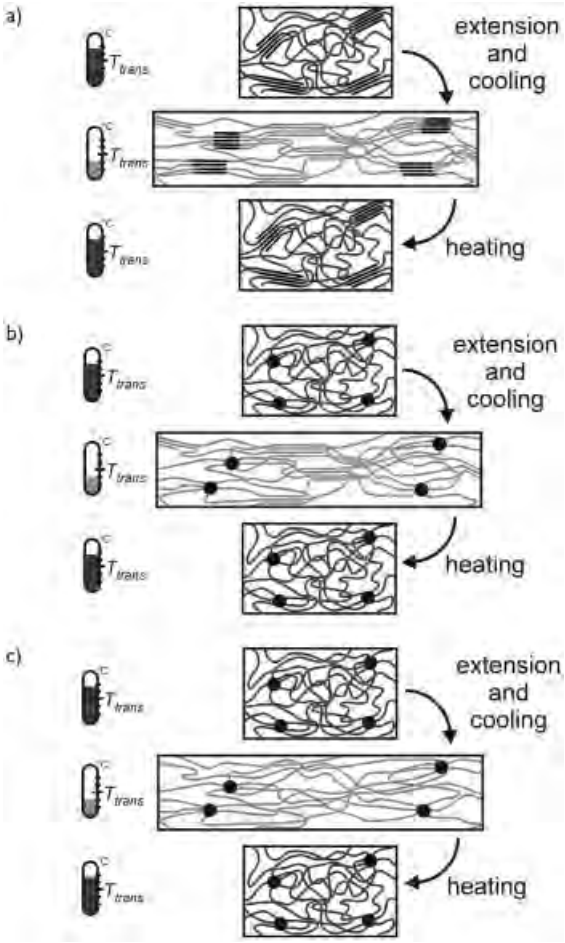

Figure 8.3 Schematic representation of the molecular mechanism of the thermally induced shape-memory effect: (a) physically crosslinked polymer network with phase-segregated domains having a crystalline or semicrystalline switching phase, (b) covalently crosslinked polymer network with crystalline or semicrystalline switching phase, and (c) covalently crosslinked polymer network with amorphous switching phase. Taken from [4]. Copyright Wiley-VCH Verlag GmbH & Co. KGaA. Reproduced with permission.

K of the examined polymer network. These cyclic, thermomechanical tests are typically performed five times. Figure 8.4b represents a three-dimensional diagram of a stress-controlled procedure. While the first cycle is used for erasing the thermal history of the polymer sample, cycles 2–5 are used for quantification of the shape-memory effect. In such a measurement, the sample is deformed at T_{high} to a maximum strain ε_m resulting in tensile stress σ_m (maximum stress) (1). The stretched specimen is then cooled to a temperature T_{low}, which is below T_{trans} (2). Several different effects of the sample behavior have to be considered, such as the

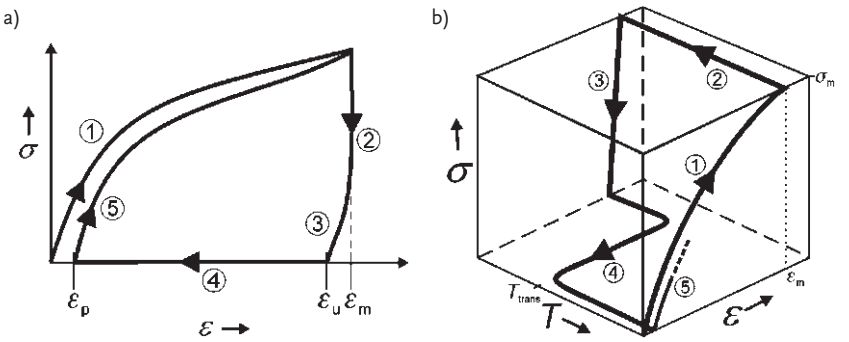

Figure 8.4 (a) ε-σ diagram of the strain-controlled programming and stress-free recovery of the shape-memory effect: (1) deformation of the sample to a maximum deformation ε_m at T_{high}; (2) cooling to T_{low} while σ_m is kept constant; (3) unloading to zero stress; (4) clamp distance is driven back to original starting distance, heating up to T_{high} while keeping $\sigma = 0$ MPa; (5) start of second cycle; (b) ε–T–σ diagram of the strain-controlled programming and stress-free recovery of the shape-memory effect: (1) stretching to ε_m at T_{high}; (2) cooling to T_{low} with constant cooling rate while σ_m is kept constant; (3) clamp distance is reduced until the stress-free state $\sigma = 0$ MPa is reached; (4) heating to T_{high} with a constant heating rate; and (5) start of the second cycle [4]. Taken from [4]. Copyright Wiley-VCH Verlag GmbH & Co. KGaA. Reproduced with permission.

strain-controlled stress-controlled

Shape fixity ratio (R_f)

$$R_f(N) = \frac{\varepsilon_u(N)}{\varepsilon_m} \quad (8.1) \qquad R_f(N) = \frac{\varepsilon_u(N)}{\varepsilon_l(N)} \quad (8.3)$$

Shape recovery ratio (R_r)

$$R_r(N) = \frac{\varepsilon_m - \varepsilon_p(N)}{\varepsilon_m - \varepsilon_p(N-1)} \quad (8.2) \qquad R_r(N) = \frac{\varepsilon_l(N) - \varepsilon_p(N)}{\varepsilon_l(N) - \varepsilon_p(N-1)} \quad (8.4)$$

Figure 8.5 Equations for the determination of R_f and R_r from cyclic, thermomechanical measurements.

change of the expansion coefficient in the vitrified or viscoelastic state or changes in volume of the sample due to crystallization effects for $T_{trans} = T_m$ [4]. After cooling, the stress is released ($\sigma = 0$ MPa) leading to the elongation ε_u (3). Finally, the sample is heated again to T_{high} and the permanent shape ε_p is recovered (4).

From these cyclic, thermomechanical tests, the values of R_r and R_f at a given strain ε_m can be determined according to the four equations in Figure 8.5.

In a strain-controlled protocol, R_f is given by the ratio of the strain in the stress-free state after the retraction of the tensile stress in the Nth cycle $\varepsilon_u(N)$ and the maximum strain ε_m (Eq. (8.1), Figure 8.5). R_f describes the ability to fix the

mechanical deformation, which has been applied during the programming process. R_r quantifies the ability of the polymer to memorize its permanent shape and it is a measure of how far the applied strain during the programming $\varepsilon_m - \varepsilon_p(N-1)$ is recovered during the SME. For that the strain that was applied during the programming in the Nth cycle, $\varepsilon_m - \varepsilon_p(N-1)$ is compared to the change in strain during the SME $\varepsilon_m - \varepsilon_p(N)$ (Eq. (8.2), Figure 8.5). The remaining strain of the samples after two successively passed cycles in the stress-free state is given by $\varepsilon_p(N-1)$ and $\varepsilon_p(N)$. In the stress-controlled protocol, R_f is represented by the ratio of the tensile strain after unloading ε_u and the strain at σ_m after cooling of the Nth cycle $\varepsilon_l(N)$ (Eq. (8.3), Figure 8.5). In such a protocol, R_r quantifies the ability of the polymer to reverse the deformation that was applied in the programming procedure $\varepsilon_l - \varepsilon_p(N-1)$ during the following shape-memory transition. For this purpose, the strain that was applied during the programming step in the Nth cycle $\varepsilon_l(N) - \varepsilon_p(N-1)$ is compared to the change of strain that occurs with the SME $\varepsilon_l(N) - \varepsilon_p(N)$ (Eq. (8.4), Figure 8.5).

8.3 Classes of Degradable SMPs

A strategy to functionalize SMP, so that they become biodegradable is the introduction of hydrolytically cleavable bonds into such polymers (see Figure 8.1) [36]. In the design of these polymers, it has to be considered that the degradation products should be either fully metabolized or excretable as fragments. This is of exceptional importance when these SMP are intended for biomedical applications. Furthermore, such degradable polymeric (bio)materials enable the application as matrix materials for controlled drug release systems that requires the exact characterization of the polymer's erosion behavior and the drug diffusion characteristics. Degradable SMPs show two types of degradation mechanisms: surface- and bulk erosion [37]. The degradation type depends on the diffusion of water into the polymer and the reactivity of the polymer functional groups (see Figure 8.1). Amorphous and crystalline segments, especially switching segments, display different degradation behavior. Amorphous segments degrade much faster due to the easier water penetration in these areas. In contrast, the penetration of water in crystalline segments is more inhibited by the dense packing of the crystalline lamellae.

In this section, an overview about degradable materials that exhibit an SME is given. SMPs can be divided into four types (see Table 8.1).

The requirements for an implant material are determined by the specific application. The key properties of degradable biomaterials are their mechanical properties, their degradation rate and degradation behavior, as well as biocompatibility and biofunctionality. Each application requires a specific combination of these properties/functions.

In the following sections, four different types of degradable SMPs are described.

Table 8.1 Overview over the four categories of SMP.

Type of netpoints of polymer network	Switching domains	Thermal transition	Example
Covalent	Crystallizable	T_m	Polymer networks from poly(ε-caprolactone) dimethacrylate [38]
Covalent	Amorphous, not crystallizable	T_g	Polymer networks from oligo[(*rac*-lactide)-*co*-glycolide] tetrol and diisocyanate [39]
Physical	Crystallizable	T_m	Polymer networks from oligo(ε-caprolactone)diole, oligo(*p*-dioxanone)diole and diisocyanate [9]
Physical	Amorphous, not crystallizable	T_g	Poly(L,L-lactide-*co*-glycolide-*co*-trimethylene carbonate) [40]

8.3.1 Covalent Networks with Crystallizable Switching Domains, $T_{trans} = T_m$

This type of polymer network consists of chain segments of homo- or copolymers and covalent netpoints. They can be prepared by (co)polymerization/poly(co)condensation of several monomers (Figure 8.6).

As a linear polyester poly(ε-caprolactone) (PCL) is hydrolytic degradable. It can be synthesized by ring-opening polymerization (ROP) of ε-caprolactone. When diols are used as initiators, macrodiols can be obtained. Covalent polymer networks can be created from these macrodiols after subsequent functionalization with polymerizable end groups, for example, dimethacrylates. These polymer networks were shown to be hydrolytically degradable and capable of an SME [38]. By the addition of a comonomer, for example, *n*-butyl acrylate, the elasticity of such polymer networks can be increased, resulting in AB copolymer networks. At the same time, T_{trans} of the network can be adjusted from 51 °C for the PCL dimethacrylate homonetwork to 44 °C for a copolymer network having 70 wt% *n*-butyl acrylate [41]. The degradability of such AB copolymer networks could be increased by the introduction of glycolide into the macrodimethacrylates [42]. The AB copolymers were prepared from poly(ε-caprolactone-*co*-glycolide) dimethacrylate and *n*-butyl acrylate as photosets. The macrodimethacrylates had a number average molecular weight (M_n) up to 13,500 g mol^{-1} and a maximum glycolide content of 21 mol%. The polymers were semicrystalline at room temperature and displayed a T_m between 18 and 53 °C. In the polymer networks, the oligo(butyl acrylate) formed the amorphous soft segment. Degradation experiments showed good hydrolytic degradability at pH 7 and 37 °C. The presence of glycolate accelerates

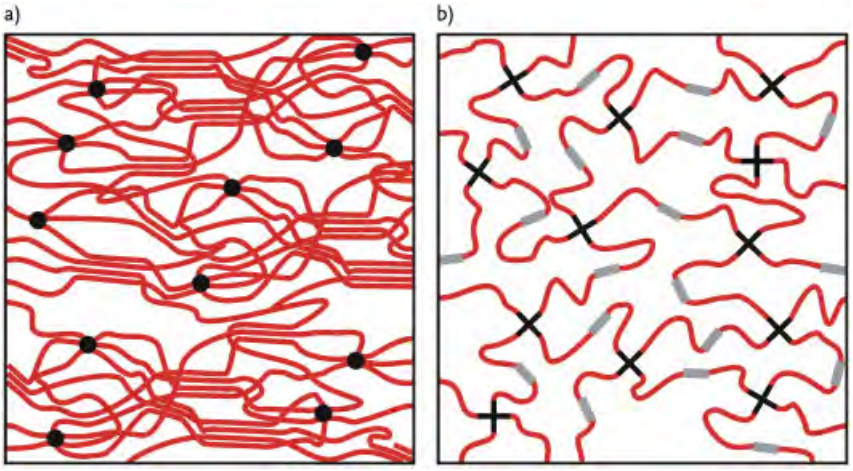

Figure 8.6 Schematic representation of covalent polymer networks. (a) Netpoints (black) consisting of acrylates or methacrylates and crystallizable switching segments (blue), for example, consisting of poly(ε-caprolactone); (b) obtained from multiarm precursors (red) acting as amorphous switching segments. The netpoints (black cross) are provided by the precursors, which were linked by small difunctional crosslinkers (gray).

the course of the hydrolytic chain scission and mass loss, and the presence of poly(*n*-butyl acrylate) segments decreases the degradation rate.

Recently, a covalent network of PCL with a percolative physical network was described [43]. Polyhedral oligosilsesquioxane (POSS) diols served as initiators for the polymerization of ε-caprolactone. The obtained oligomers were acrylated and crosslinked with a tetrathiol by photopolymerization to form a so-called double network. Here, the POSS moieties, which were located in side chains, provided a physical network, while the acrylate groups built a covalent polymer network, and the PCL chain segments contributed the switching domains. The content of POSS was varied from 22 to 47 wt% in the networks. Higher POSS content resulted in two distinct rubbery plateaus during the thermomechanical tests. T_m of the PCL moieties ranged from 39 to 47 °C and T_m of the POSS moieties from 86 to 69 °C depending on the content. Applications in tissue engineering and drug delivery were thought to be possible.

Poly[(3-hydroxybutyrate)-*co*-(3-hydroxyvalerate)], which was produced by bacteria, displayed an SME. The temporary shape was fixed by induced formation of hard domains by orientation via stretching the material [44]. The material had a very broad melting transition from approximately 37 to 115 °C and an elongation at break (ε_R) of 700%.

Recently, a stent made of an SMP from chitosan films crosslinked with an epoxy compound (ethylene glycol diglycidyl ether), which was blended with polyethylene glycol and glycerol was reported [45]. Generally, chitosan-based films

are brittle because of their high crystallinity. Blending of the SMP with polyethylene glycol (M_n = 400,000 g mol^{-1}) reduced the crystallinity and enabled shape-memory properties of the material. The SME could be repeated several times and could be controlled by the hydration or dehydration of the SMP. When immersed in an aqueous buffer solution of 37 °C, the material recovered its permanent shape within 150 s. The degradability of the material was investigated in enzymatic degradation studies in lysozyme solution for 10 weeks. The material was shown to be degradable, but degradability decreased with increasing crosslinking density.

8.3.2
Covalent Networks with Amorphous Switching Domains, $T_{trans} = T_g$

In covalently crosslinked polymer networks, the general parameters for controlling the shape-memory behavior are the nature of the switching segments influencing the characteristics of the SME such as T_{switch} and the crosslink density influencing the mechanical properties.

Completely amorphous polymer networks with a thermally induced SME are described in reference [46], but were not originally developed for medical applications and are not hydrolytically degradable. Amorphous, biodegradable SMP networks could be prepared by coupling well-defined star-shaped hydroxy-telechelic polyesters with a low-molecular-weight junction unit (diisocyanate) [39]. The copolyester segments were formed by copolymerization of diglycolide and *rac*-dilactide and yielded the oligo[(*rac*-lactide)-*co*-glycolide] by ROP. The application of 1,1,1-tris(hydroxymethyl)ethane and pentaerythrite as initiators resulted in trifunctional or tetrafunctional star-shaped precursors, respectively. The mechanical properties of such polymer networks could be substantially enhanced by the introduction of an additional amorphous phase being immiscible with the first amorphous component. Incorporation of poly(propylene glycol) led to microscopic phase segregation within the amorphous networks and thus resulted in two distinct glass transitions with one T_g between –59 and –25 °C and the second T_g between 39 and 53 °C as well as good elastic properties at ambient temperature with ε_R up to 500%. The mechanical properties could be controlled by independently altering the two parameters, content and molecular weight of the poly(propylenglycol) segment [47].

The substitution of the diglycolide comonomer by other cyclic diesters in the synthesis of hydroxytelechelic copolyesters was shown to be another parameter to control T_{trans} of such amorphous polymer networks [48].

Transparent and hydrolytically degradable SMP networks with $T_{trans} = T_g$ based on acrylate chemistry could be obtained by UV polymerization of poly[(L-lactide)-*ran*-glycolide] dimethaycrylates (PLGDMA) [49]. Hydroxy telechelic poly[(L-lactide)-*ran*-glycolide]s (PLG) M_n between 1000 and 5700 g mol^{-1} were prepared by ROP from L,L-dilactide, diglycolide, and ethylene glycol as initiator using dibutyltin oxide as the catalyst. Subsequent functionalization of the PLG with methacryloyl chloride resulted in terminal methacrylate groups. T_g was shown to be almost

constant at about 55 °C. Mechanical properties of these polymer networks below and above T_g differed significantly. The storage modulus E' determined by dynamic mechanical analysis at varied temperature (DMTA) was 3080 MPa at room temperature with ε_R = 43% and 8 MPa at 80 °C with ε_R = 130%. The mechanical properties at temperatures higher than T_g depended on crosslinking density. A hydrolytic degradation in bulk could be expected according to the described behavior for PLG [50]. Excellent shape-memory properties with R_r close to 100% were obtained during tests under stress-control.

Phase-separated, amorphous, and degradable block copolymer networks were also prepared by photo crosslinking of the linear ABA triblock precursors poly(*rac*-lactide)-*b*-poly(propylene oxide)-*b*-poly(*rac*-lactide)dimethacrylate [51]. A polypropyleneglyocol (B-block) with M_n = 4000 g mol^{-1} was used as a macroinitiator for poly(*rac*-lactide) synthesis, whereas poly(*rac*-lactide) blocks (A-blocks) with M_n of 2000, 4000, and 6000 g mol^{-1} were obtained. Thus, the length of the macrodimethacrylates precursors was systematically varied and SMP networks with different mechanical properties were synthesized. The T_g of the phase provided by the poly(propylene oxide) was obtained at −50 °C. An additional transition associated to the mixed phase between the phase transition resulting from the poly(propylene oxide) and the poly(*rac*-lactide) as well as the phase transition from the poly(propylene oxide) were observed, when M_n of the macro-dimethacrylate precursors was <10 g mol^{-1}. A distinct phase separation of the resulting polymer networks could be observed for macrodimethacrylate precursors with M_n > g mol^{-1}. Values of ε_R from 70% to 219% could be achieved and the polymers displayed R_f values between 92% and 96% and R_r values from 87% to values over 99%, which increased with increasing poly(*rac*-lactide) content. Potential biomedical applications are intelligent implants or smart drug delivery systems.

8.3.3
Physical Networks with Crystallizable Switching Domains, $T_{trans} = T_m$

An important group of this type of SMPs is based on linear multiblock copolymers. Phase-segregated domains have to be formed by different segments being represented by different types of blocks within the linear polymer chains. A T_{trans} related to a T_m is obtained when the domains of the switching segment are crystallizable. The polymer blocks could be biodegradable polyesters or polyethers. Prominent examples for this type of multiblock copolymers are polyesterurethanes (PEUs). In such PEUs, the polyurethane segments are acting as hard segments, while the polyester segments, for example, PCL, are representing the switching segments (Figure 8.7). Thermoplastic SMP can be synthesized by direct coupling of presynthesized polymer blocks with a reactive linker, by applying the prepolymer method, or by melt blending. The application of the prepolymer method enabled the production of thermoplastic polyurethane elastomers on an industrial scale. In this process, isocyanate-terminated prepolymers are obtained by reaction of hydroxytelechelic oligoesters or -ethers with an excess of a low-molecular-weight diisocyanate. Biocompatible and simultaneously biodegradable multiblock copolymers

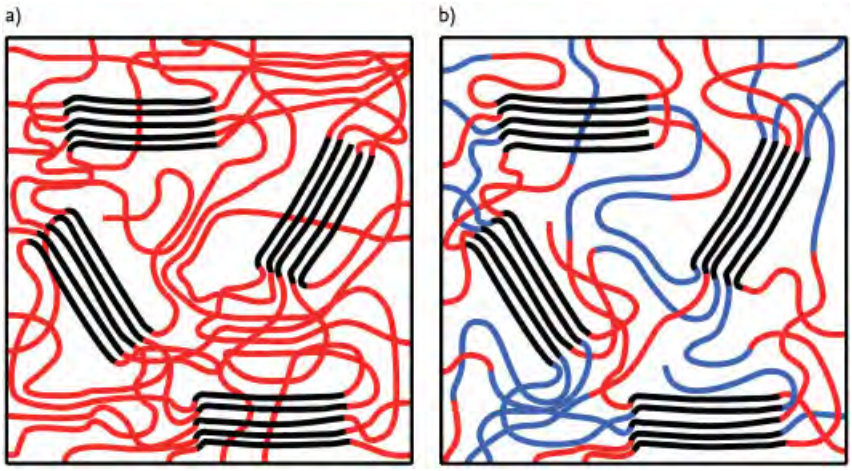

Figure 8.7 Schematic representation of physically crosslinked polymer networks: (a) polymer network with hard segments (black) and crystallizable switching segments (red); (b) multiblock copolymer with hard segment (black) and two amorphous switching segments (red, blue).

with shape-memory properties could be synthesized via co-condensation of macrodiols from poly(*p*-dioxanone) (PPDO) and PCL using an isomeric mixture of 1,6-diisocyanato-2,2,4-trimethylhexane and 1,6-diisocyanato-2,4,4-trimethylhexane as a bifunctional coupling agent [9]. The required diols were synthesized by ROP of the cyclic esters [52]. In these multiblock copolymers, named PDC, PPDO with the higher T_m was chosen as the hard segment to provide the physical crosslinks determining the permanent shape, while the crystallizable PCL is acting as switching segment. The mechanical properties strongly depend on the hard segment content. Hard segment contents of the synthesized polymers ranged from 0 to 83 wt%. The multiblock copolymers were elastic at room temperature and exhibited ε_R values up to 1000%. An increase of the PPDO amount resulted in a stiffer polymer and a decrease of the corresponding ε_R. R_f between 98% and 99.5% were determined throughout all cycles, while R_r depended on the cycle number and gradually approached values near 100%.

The same type of polymer as a blend with a poly(alkylene adipate) as mediator segment to promote the miscibility of the other segments showed also shape-memory properties, was biodegradable and is therefore a candidate for biomedical applications [53].

Phase-segregated PEUs prepared from PCL diol, ethylene glycol, and 2,4-toluene diisocyanate as linker showed shape-memory behavior and due to the PCL are biodegradable [54]. A tensile deformation of 300% was possible and R_r values between 94% and 100% could be determined. By adjusting the molecular weight of the PCL diol and the hard-to-soft ratio, the switching temperature could be adjusted to the range of 37–42 °C. In multiblock copolymers having PCL switching

segments and POSS moieties in the polyurethane hard segments, a tremendous increase in the elasticity above T_{trans} was determined, which was attributed to physical crosslinks formed in the hard domains through POSS crystallization [55]. Recently, the degradation characteristics of crystalline multiblock copolymers had been investigated on SMP urethanes (SMPU) based on poly(adipate)diol ($M_w = 3500\,g\,mol^{-1}$) as switching segment and a hard segment derived from methylene-bis(4-phenylisocyanate) (MDI) and butanediol (BD). The degradation process could be divided into three phases: an induction phase, a phase of continuous degradation, and a phase of accelerated degradation. R_r remained fairly constant during phase one and decreased slowly during phase two. The increase in crystallinity in phase two was accompanied by an increase in R_f [56].

During the hydrolytic degradation of polyester segments, carboxylic acids are generated. In contrast, when some of the ester functional groups are replaced by peptide segments as in polydepsipeptides, the carboxylic acids can be directly buffered by the amino functions, which are also generated during degradation. The substitution of a polyester segment by polydepsipeptide segment in multiblock copolymers is thought to combine advantageous degradation behavior of the depsipeptide segment with the shape-memory capability of multiblock copolymers with the PCL switching segment. Thermoplastic multiblock copolymers with polydepsipeptide- and PCL segments providing shape-memory capability were synthesized via coupling of the depsipeptide oligo[3-(*R*)-isobutylmorpholine-2,5-dione]diol (PIBMD) and PCL diol ($M_n = 2900\,g\,mol^{-1}$) using TMDI [57]. In these polymer materials, the switching domains were formed by the PCL block, while the domains determining the permanent shape were formed by the polydepsipeptide segments. The shape-memory properties of such a thermoplastic multiblock copolymer with 50 wt% of PCL segments yielded in R_f and R_r values of more than 96% for all cycles, a T_{sw} around body temperature, and an ε_R value of 680%. The degradation behavior shows a mass loss of 12 wt% at 37 °C over 70 days in aqueous buffer solution.

Other physically crosslinked networks based on PCL and α-cyclodextrines (α-CD) form partial inclusion complexes using the molecular recognition of CDs. The T_m of PCL makes it suitable for clinical applications [58], but the transition temperature of the complex is around 60 °C. PCL with a molecular weight of $80{,}000\,g\,mol^{-1}$ was applied because polymers with lower molecular weight formed complete inclusion complexes with the α-CD resulting in a crystalline powder. The material was obtained by solvent casting at 70 °C with DMF. It was important to keep the theoretical mass proportion of the inclusion complexes between 30% and 50%, otherwise the resulting materials dissolved during purification or became too brittle. The R_r value was found to be between 95% (for 30% inclusion ratio) and 90% (for 50% inclusion ratio) and R_f values between 92% and 83% were obtained for the complexes. Biodegradability was evaluated by an enzymatic test at 37 °C.

A hyperbranched SMPU was synthesized from poly(butylenes adipate)glycol (PBAG), a hyperbranched polyester (Boltron H30), and MDI [59]. The synthesis was accomplished by a two-step process, first functionalization of PBAG with

MDI, which was followed by the addition of Boltron H30 as a chain extender. The polyurethane with 25 wt% of hard segment showed the best results in shape-memory behavior. The R_r was 96–98% for a hard segment content of 15–35 wt%. A higher content disturbed the crystallization of the PBAG soft segment.

8.3.4 Physical Networks with Amorphous Switching Domains, $T_{trans} = T_g$

In this type of SMP, the switching temperature is related to a T_g. Examples for biodegradable SMP having $T_{trans} = T_g$ are polyetherurethanes synthesized by applying the prepolymer method leading to a hard segment from MDI, BD, and poly(tetramethyleneoxide) (PTHF) or polyethylene adipate as second segment [4]. These polymers form predominantly a mixed domain acting as switching phase (Figure 8.7b). The quality of phase separation between the polyurethane segments and the polyetherurethane is determined by the molecular weight of the polytetrahydrofurandiols used as precursors. In a commercially available polyetherurethane synthesized from methylene bis(*p*-cyclohexyl isocyanate) (H12 MDI), 1,4-butanediol (BD), and PTHF diol (Tecoflex®), T_g is at 74 °C. This material is used in artificial hearts, wound dressings, and pacemaker leads [60]. Determination of shape-memory properties revealed R_f values of 100% and R_r values of 80% after the third cycle at $\varepsilon_m = 50\%$. The incorporation of silica-coated magnetic nanoparticles of iron(III)oxide core into Tecoflex® enabled the remote actuation of the thermally induced SME in alternating magnetic fields [28].

A terpolymer from L,L-dilactide, diglycolide, and trimethylene carbonate prepared by ROP with $Zr(Acac)_4$ as catalyst exhibited a single-phase amorphous material with no evidence of phase separation [61]. Usually, physically crosslinked SMP networks display at least two phases with distinct thermal transitions. Polymers prepared by random polymerization of the three monomers resulted in materials having values of M_n between 25,000 and 54,000 g mol^{-1} and PDI values between 2.0 and 2.3. R_r values from 89 to 95% at initial recovery temperatures between 38 to 42 °C enabled applications in the biomedical field. The T_g of the terpolymers changed with the composition in a predictable manner and followed a trend based on the relative amount of the three units, but stayed always close to body temperature. A further advantage is the use of a zirconium complex as initiator. This compound is significantly less toxic compared to common stannous initiator and inert in human metabolic processes.

To overcome the drawback of the low stiffness of SMP for bone regeneration applications, addition of fibers or particles is necessary to reinforce the polymers. Composites of hydroxyapatite (HAP) with poly(D,L-lactide) (PDLLA) also showed shape-memory properties which are improved compared to pure PDLLA [62]. PDLLA was synthesized by ROP and afterwards uniformly mixed with HAP particles. T_g was increasing from 54 °C for pure PDLLA to 59 °C for a 1:1 mixture. For a mixture of PDLLA/HAP 3:1 having a T_g of 53 °C, the storage modulus (E') at 23 °C was 3220 MPa and 29.6 MPa at 83 °C. The recovery rates of the materials were all

above 95%. Comparable behavior was shown by a PDLLA composite with β-tricalcium phosphate composite [63].

8.4 Applications of Biodegradable SMPs

During the last few years, the research field of SMPs as materials for biomedical applications has grown rapidly. SMPs were widely investigated in specific medical instruments as highly recoverable and convenient materials for minimally invasive surgery [9], in drug delivery systems [64], vascular surgery [65], implantable devices [35], and intracranial aneurysm surgery [66]. The clinical trend toward MIS techniques sets new requirements for materials to be used as a matrix of medical devices [67]. This technique would benefit from the implantation of small objects that unfold to bulky devices of desired shape and functionality. In the following text, examples for medical devices based on biodegradable SMP will be presented and briefly discussed. Overviews for the use of SMPs for medical devices can be found in previous reviews [68, 69].

8.4.1 Surgery and Medical Devices

Depending on the respective application, implants should provide a supportive function and mechanical strength over a long period of time or only temporarily, whereas the material should then biodegrade and disappear from the site of application. So far, the suggested SMP medical devices are only based on thermosensitive SMPs. Besides triggering the shape recovery by direct exposure to heat (e.g., body temperature, flushing with warm water), indirect heating by light absorption of near-infrared dyes loaded into the material is an intensively evaluated approach particularly for intravascular applications [70].

Major targets for the evaluation of biodegradable SMPs in medical devices in the field of cardiovascular applications are stents [8, 65]. Stents are used to maintain the internal lumen of blood vessels when local flow constrictions were removed by cardiovascular intervention. Stents have to be inserted in a shape with a small outer diameter, and then subsequently expand and apply pressure against the surrounding tissue. Fully degradable stents are believed to be the future in stent technology [71]. However, so far, most studies on SMPs as stent matrices have been conducted with nondegradable SMPs. Only in some cases, partially degradable materials employing degradable polyester segments were evaluated [12].

For optimal healing after surgery with minimal scar formation, wounds have to be closed by applying a defined pressure to the wound lips. A programmed suture made from SMPs exhibiting a T_{trans} around body temperature has the capacity to exert a controllable pressure on the wound edges, holding the wound closed even after potential inflammatory swelling decayed. An example for such a suture is

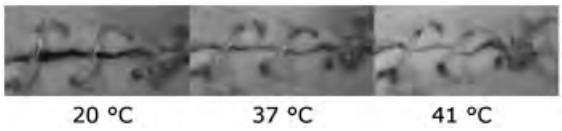

Figure 8.8 Picture series of a degradable suture from a multiblock copolymer with crystallizable switching segments used for wound closure. Taken from [9]. Reprinted with permission from AAAS, USA.

shown in Figure 8.8. The degradability of the material increases the patients' comfort as the second surgery for removal of the suture can be avoided and the risk for infections is decreased.

Other important fields of currently developed SMP applications are aneurysm treatment and clot removal devices. Aneurysms may be associated with potentially lethal rupture or uncontrolled aggregation of blood clots, which could embolize peripheral tissue when removed from the aneurysm into the blood stream. Among different treatment options, commonly used or suggested strategies that rely on endovascular implantation of medical devices include the implantation of vessel prostheses in aortic aneurysm [72, 73]. From first simulation data, SMP foams can be considered to be a promising treatment option of intracranial aneurysm, since they may reduce the risk of intraoperative rupture [74]. Preliminary *in vivo* data in dogs for aneurysms of the common carotid artery showed a successful closure, at least macroscopically in this healing vessel model [10].

For the treatment of cerebral ischemia in stroke patients, mechanical removal of intravascular blood clots has been advantageous at timepoints several hours after the onset of the stroke, where clot-dissolving standard therapies are no longer effective. A microcatheter system was introduced that is guided to the occluded vessel and passed beyond the thrombus. A nitinol wire is advanced through the catheter, deploys at the end of the catheter in a spring-like manner to a helical corkscrew-shape, and captures the clot [75]. Similar to this strategy, a corkscrew system [76] and an umbrella device [70] have been designed using commercially available covalently crosslinked thermosensitive SMP networks [77].

8.4.2 Drug Release Systems

The application of degradable polymeric biomaterials as matrix materials for pharmaceutically active agents enables stimuli-sensitive controlled drug release systems. The concept of a controlled and sustained release of drugs from biodegradable implants was developed more than 30 years ago [78]. Drugs, incorporated in a polymer, should be delivered in a controlled manner in predefined rates. In contrast to daily peroral medication, for example, with tablets, such implants should reduce the frequency of administration and provide a constant level of the desired drug in the body over an extended period of time. SMP materials as carrier for the drug would allow the implantation of bulky devices by MIS and fixation of

such a device at the place of application. This has led to multifunctional materials for biomedical applications, which combine biodegradability, controlled drug release, and shape-memory capability. After implantation of a medical device, the SME can affect a fixation of the device at the site of implantation. Subsequently, the controlled release of the loaded drug is used for treating infections, reducing inflammatory responses, or, potentially, supporting regeneration processes. Finally, the degradation of the matrix can avoid a second surgery for removal of the implant.

In multifunctional SMPs that involve controlled drug release, specific processes in synthesis, processing, and programming have to be applied to enable each of the functionalities. Key for a release of bioactive molecules is their incorporation into the polymer matrix. Drug incorporation into the matrix can principally be achieved by soaking of the synthesized matrix in a drug solution and a subsequent drying step, or alternatively by mixing of defined amounts of drug with polymer network precursors and subsequent crosslinking. The latter method often allows higher drug loading, but is limited by the chemical stability of the drug under the crosslinking conditions. Drug release from polymer matrices is most often ruled either by diffusion or by degradation of the matrix. Diffusion-controlled release from a degradable matrix can, for example, be achieved for small water-soluble molecules from bulk-eroding materials [79–81]. Alternatively, the use of surface-eroding materials such as polyanhydrides [82] or poly(orthoesters) [83] allows an erosion-controlled drug release. So far, only a few systems representative for triple functional materials combining biodegradability, SME, and controlled drug release have been published. All of them belong to the bulk eroding polyesters with a diffusion-controlled release. However, type and ratio of the monomers as well as network architectures resulted in quite different capabilities of the networks.

First examples for triple functional SMPs were polymer networks from poly(*ε*-caprolactone-*co*-glycolide)dimethacrylate. In these semicrystalline networks, hydrophobic and hydrophilic drugs could be incorporated either by swelling of the final networks in an organic solvent saturated with the respective drug or by mixing defined amounts of the drug with the network precursors followed by irradiation (*in situ* incorporation) [84]. A semicrystalline polymer network was chosen so that the crystalline phases of the networks were used for the fixation of the temporary shape, while drug molecules should predominantly be incorporated in the amorphous phases without having a too strong influence on the melting point of the polymer crystallites or the shape fixation and recovery [85]. Large amounts of drug decreased the elongation at break of the networks, which reduced their programmability. In materials with high crystallinity in the drug-free state, no effect of drug loading on the thermomechanical properties and shape-memory functionality was observed.

Drug-loaded networks, which were shown to have high shape-fixity and shape-recovery, were subjected to hydrolytic degradation compared with drug-free samples. It was found that a diffusion-controlled release was realized before erosion of the matrix would have led to changes in the rate of drug release. Furthermore, independence of polymer functionalities could be demonstrated.

However, only limited amounts of drug could be incorporated by swelling (<1 wt%), which was theoretically high enough to ensure pharmacological efficiency of the model drugs but might be necessary to be increased for other drugs.

It was assumed that a higher drug loading by swelling can be achieved in fully amorphous SMPs such as the star-shaped PLG networks described above. In contrast to semicrystalline materials, the entire matrix is amorphous and therefore accessible for drugs [86]. Furthermore, crystallization is not required for shape fixation, thus allowing a wider variability for network composition and network architecture. Also, loading may not impact shape fixation. However, drug molecules can possibly act as softeners and reduce the T_g of amorphous SMPs, which can result in an unwanted shift in T_{switch}. Overall, SMPs as a technology platform can be envisaged to have a high potential for transfer into biomedical applications requiring biodegradable, multifunctional materials due to the generality of the underlying fundamental principles of the SME and the synthetic preparation of SMP network architectures as polymer systems, in which functions and properties can be tuned in a wide range by only small variations of their chemical structure. While basic research in SMPs is progressing rapidly, broadening the application potential of the SMP platform besides biomedical applications, the polymer system approach enables existing SMPs to be tailored to the challenging demands of the medicinal sector.

References

1 Rainer, W.C., Redding, E.M., Hitov, J.J., Sloan, A.W., and Steward, W.D. (1964) Heat-shrinkable polyethylene. US Patent, 3144398.

2 Arditti, S.J., Avedikian, S.Z., and Bernstein, B.S. (1971) Articles with Polymeric Memory US Patent, 3563973.

3 Charlesby, A. (1960) *Atomic Radiation and Polymers*, Pergamon Press, New York, pp. 198–257.

4 Lendlein, A. and Kelch, S. (2002) Shape-memory polymers. *Angew. Chem. Int. Ed.*, **41** (**12**), 2034–2057.

5 Mondal, S. and Hu, J.L. (2006) Temperature stimulating shape memory polyurethane for smart clothing. *Indian J. Fibre Text. Res.*, **31** (**1**), 66–71.

6 Hu, J. (2007) *Shape Memory Polymers and Textiles*, England Woodhead Publishing Limited, Cambridge.

7 Gall, K., Mikulas, M., Munshi, N.A., Beavers, F., and Tupper, M. (2000) Carbon fiber reinforced shape memory polymer composites. *J. Intell. Mater. Syst. Struct.*, **11** (**11**), 877–886.

8 Wache, H.M., Tartakowska, D.J., Hentrich, A., and Wagner, M.H. (2003) Development of a polymer stent with shape memory effect as a drug delivery system. *J. Mater. Sci. Mater. Med.*, **14** (**2**), 109–112.

9 Lendlein, A. and Langer, R. (2002) Biodegradable, elastic shape-memory polymers for potential biomedical applications. *Science*, **296** (**5573**), 1673–1676.

10 Metcalfe, A., Desfaits, A.C., Salazkin, I., Yahia, L., Sokolowski, W.M., and Raymond, J. (2003) Cold hibernated elastic memory foams for endovascular interventions. *Biomaterials*, **24** (**3**), 491–497.

11 Behl, M. and Lendlein, A. (2007) Actively moving polymers. *Soft Matter*, **3**, 58–67.

12 Bellin, I., Kelch, S., Langer, R., and Lendlein, A. (2006) Polymeric triple-shape materials. *Proc. Natl. Acad. Sci. USA*, **103** (**48**), 18043–18047.

13 Bellin, I., Kelch, S., and Lendlein, A. (2007) Dual-shape properties of

triple-shape polymer networks with crystallizable network segments and grafted side chains. *J. Mater. Chem.*, **17** (**28**), 2885–2891.
14 Behl, M., Bellin, I., Kelch, S., Wagermaier, W., and Lendlein, A. (2009) One-step process for creating triple-shape capability of AB polymer networks. *Adv. Funct. Mater.*, **19** (**1**), 102–108.
15 Kolesov, I.S. and Radusch, H.-J. (2008) Multiple shape-memory behavior and thermal-mechanical properties of peroxide cross-linked blends of linear and short-chain branched polyethylenes. *Express Polym. Lett.*, **2** (**7**), 461–473.
16 Pretsch, T. (2010) Triple-shape properties of a thermoresponsive poly(ester urethane). *Smart Mater. Struct.*, **19** (**1**), 015006.
17 Xie, T. (2010) Tunable polymer multi-shape memory effect. *Nature*, **464** (**7286**), 267–270.
18 Zotzmann, J., Behl, M., Feng, Y., and Lendlein, A. (2010) Copolymer networks based on poly(ω-pentadecalactone) and poly(ω-caprolactone)segments as a versatile triple-shape polymer system. *Adv. Funct. Mater.*, **20** (**20**), 3583–3594.
19 Behl, M. and Lendlein, A. (2010) Triple-shape materials. *J. Mater. Chem.*, **20** (**17**), 3335–3345.
20 Beloshenko, V.A., Varyukhin, V.N., and Voznyak, Y.V. (2005) The shape memory effect in polymers. *Russ. Chem. Rev.*, **74** (**3**), 265–283.
21 Behl, M. and Lendlein, A. (2007) Shape-memory polymers. *Mater. Today*, **10** (**4**), 20–28.
22 Mather, P.T., Luo, X.F., and Rousseau, I.A. (2009) Shape memory polymer research. *Annu. Rev. Mater. Res.*, **39**, 445–471.
23 Behl, M., Zotzmann, J., and Lendlein, A. (2010) Shape-memory polymers and shape-changing polymers. *Adv. Polym. Sci.*, **226**, 1–40.
24 Koerner, H., Price, G., Pearce, N.A., Alexander, M., and Vaia, R.A. (2004) Remotely actuated polymer nanocomposites–stress-recovery of carbon-nanotube-filled thermoplastic elastomers. *Nat. Mater.*, **3** (**2**), 115–120.
25 Lendlein, A., Jiang, H.Y., Jünger, O., and Langer, R. (2005) Light-induced shape-memory polymers. *Nature*, **434** (**7035**), 879–882.
26 Cho, J.W., Kim, J.W., Jung, Y.C., and Goo, N.S. (2005) Electroactive shape-memory polyurethane composites incorporating carbon nanotubes. *Macromol. Rapid Commun.*, **26** (**5**), 412–416.
27 Leng, J.S., Lv, H.B., Liu, Y.J., and Du, S.Y. (2007) Electroactivate shape-memory polymer filled with nanocarbon particles and short carbon fibers. *Appl. Phys. Lett.*, **91** (**14**), 144105.
28 Mohr, R., Kratz, K., Weigel, T., Lucka-Gabor, M., Moneke, M., and Lendlein, A. (2006) Initiation of shape-memory effect by inductive heating of magnetic nanoparticles in thermoplastic polymers. *Proc. Natl. Acad. Sci. USA*, **103** (**10**), 3540–3545.
29 Buckley, P.R., McKinley, G.H., Wilson, T.S., Small, W., Benett, W.J., Bearinger, J.P., McElfresh, M.W., and Maitland, D.J. (2006) Inductively heated shape memory polymer for the magnetic actuation of medical devices. *IEEE Trans. Biomed. Eng.*, **53** (**10**), 2075–2083.
30 Razzaq, M.Y., Anhalt, M., Frormann, L., and Weidenfeller, B. (2007) Thermal, electrical and magnetic studies of magnetite filled polyurethane shape memory polymers. *Mater. Sci. Eng. Struct. Mater. Prop. Microstruct. Process.*, **444** (**1-2**), 227–235.
31 Kumar, U.N., Kratz, K., Wagermaier, W., Behl, M., and Lendlein, A. (2010) Non-contact actuation of triple-shape effect in multiphase polymer network nanocomposites in alternating magnetic field. *J. Mater. Chem.*, **20** (**17**), 3404–3415.
32 Yang, B., Huang, W.M., Li, C., and Chor, J.H. (2005) Effects of moisture on the glass transition temperature of polyurethane shape memory polymer filled with nano-carbon powder. *Eur. Polym. J.*, **41** (**5**), 1123–1128.
33 Lendlein, A. and Kelch, S. (2005) Degradable, multifunctional polymeric biomaterials with shape-memory. *Mater. Sci. Forum*, **492-493**, 219–223.
34 Behl, M., Razzaq, M.Y., and Lendlein, A. (2010) Multifunctional shape-memory

polymers. *Adv. Mater.*, **22** (**31**), 3388–3410.
35 Lendlein, A. and Kelch, S. (2005) Shape-memory polymers as stimuli-sensitive implant materials. *Clin. Hemorheol. Microcirc.*, **32** (**2**), 105–116.
36 Weigel, T., Schinkel, G., and Lendlein, A. (2006) Design and preparation of polymeric scaffolds for tissue engineering. *Expert Rev. Med. Devices*, **3** (**6**), 835–851.
37 Brannon-Peppas, L. (1997) Polymers in controlled drug delivery. *Med. Plast. Biomater.*, **4**, 34–44.
38 Lendlein, A., Schmidt, A.M., Schroeter, M., and Langer, R. (2005) Shape-memory polymer networks from oligo(epsilon-caprolactone)dimethacrylates. *J. Polym. Sci. [A]*, **43** (**7**), 1369–1381.
39 Alteheld, A., Feng, Y.K., Kelch, S., and Lendlein, A. (2005) Biodegradable, amorphous copolyester–urethane networks having shape-memory properties. *Angew. Chem. Int. Ed.*, **44** (**8**), 1188–1192.
40 Zini, E., Scandola, M., Dobrzynski, P., Kasperczyk, J., and Bero, M. (2007) Shape memory behavior of novel (L-lactide-glycol ide-trimethylene carbonate) terpolymers. *Biomacromolecules*, **8** (**11**), 3661–3667.
41 Lendlein, A., Schmidt, A.M., and Langer, R. (2001) AB-polymer networks based on oligo(epsilon-caprolactone) segments showing shape-memory properties. *Proc. Natl. Acad. Sci. USA*, **98** (**3**), 842–847.
42 Kelch, S., Steuer, S., Schmidt, A.M., and Lendlein, A. (2007) Shape-memory polymer networks from oligo[(epsilon-hydroxycaproate)-*co*-glycolate] dimethacrylates and butyl acrylate with adjustable hydrolytic degradation rate. *Biomacromolecules*, **8** (**3**), 1018–1027.
43 Lee, K.M., Knight, P.T., Chung, T., and Mather, P.T. (2008) Polycaprolactone-POSS chemical/physical double networks. *Macromolecules*, **41** (**13**), 4730–4738.
44 Kim, Y.B., Chung, C.W., Kim, H.W., and Rhee, Y.H. (2005) Shape memory effect of bacterial poly[(3-hydroxybutyrate)-*co*-(3-hydroxyvalerate)]. *Macromol. Rapid Commun.*, **26** (**13**), 1070–1074.
45 Chen, M.C., Tsai, H.W., Chang, Y., Lai, W.Y., Mi, F.L., Liu, C.T., Wong, H.S., and Sung, H.W. (2007) Rapidly self-expandable polymeric stents with a shape-memory property. *Biomacromolecules*, **8** (**9**), 2774–2780.
46 Takeda, K., Akiyama, M., and Yamamizu, T. (1988) Shape-memory pore structure in porous crosslinked polystyrenes. *Angew. Makromol. Chem.*, **157**, 123–136.
47 Zotzmann, J., Alteheld, A., Behl, M., and Lendlein, A. (2009) Amorphous phase-segregated copoly(ether) esterurethane thermoset networks with oligo(propylene glycol) and oligo[(*rac*-lactide)-*co*-glycolide] segments: synthesis and characterization. *J. Mater. Sci. Mater. Med.*, **20**, 1815–1824.
48 Lendlein, A., Zotzmann, J., Feng, Y., Alteheld, A., and Kelch, S. (2009) Controlling the switching temperature of biodegradable, amorphous, shape-memory poly(*rac*-lactide)urethane networks by incorporation of different comonomers. *Biomacromolecules*, **10**, 975–982.
49 Choi, N.Y. and Lendlein, A. (2007) Degradable shape-memory polymer networks from oligo[(L-lactide)-*ran*-glycolide]dimethacrylates. *Soft Matter*, **3** (**7**), 901–909.
50 Li, S.M., Garreau, H., and Vert, M. (1990) Structure-property relationships in the case of the degradation of massive poly(α-hydroxy acids) in aqueous media. Part 2. Degradation of lactide–glycolide copolymers: PLA37.5GA25 and PLA75GA25. *J. Mater. Sci. Mater. Med.*, **1** (**3**), 131–139.
51 Choi, N.Y., Kelch, S., and Lendlein, A. (2006) Synthesis, shape-memory functionality and hydrolytical degradation studies on polymer networks from poly(*rac*-lactide)-*b*-poly(propylene oxide)-*b*-poly(*rac*-lactide) dimethacrylates. *Adv. Eng. Mater.*, **8** (**5**), 439–445.
52 Grablowitz, H. and Lendlein, A. (2007) Synthesis and characterization of,-dihydroxy-telechelic oligo(*p*-dioxanone). *J. Mater. Chem.*, **17** (**38**), 4050–4056.
53 Behl, M., Ridder, U., Feng, Y., Kelch, S., and Lendlein, A. (2009) Shape-memory capability of binary multiblock copolymer blends with hard and switching domains

provided by different components. *Soft Matter*, **5** (**3**), 676–684.
54 Ping, P., Wang, W.S., Chen, X.S., and Jing, X.B. (2005) Poly(epsilon-caprolactone) polyurethane and its shape-memory property. *Biomacromolecules*, **6** (**2**), 587–592.
55 Knight, P.T., Lee, K.M., Qin, H., and Mather, P.T. (2008) Biodegradable thermoplastic polyurethanes incorporating polyhedral oligosilsesquioxane. *Biomacromolecules*, **9** (**9**), 2458–2467.
56 Pretsch, T., Jakob, I., and Müller, W. (2009) Hydrolytic degradation and functional stability of a segmented shape memory poly(ester urethane). *Polym. Degrad. Stab.*, **94** (**1**), 61–73.
57 Feng, Y.K., Behl, M., Kelch, S., and Lendlein, A. (2009) Biodegradable multiblock copolymers based on oligodepsipeptides with shape-memory properties. *Macromol. Biosci.*, **9** (**1**), 45–54.
58 Luo, H., Liu, Y., Yu, Z., Zhang, S., and Li, B. (2008) Novel biodegradable shape memory material based on partial inclusion complex formation between α-cyclodextrin and poly(ε-caprolactone). *Biomacromolecules*, **9** (**10**), 2573–2577.
59 Cao, Q. and Liu, P. (2006) Structure and mechanical properties of shape memory polyurethane based on hyperbranched polyesters. *Polym. Bull.*, **57** (**6**), 889–899.
60 Guignot, C., Betz, N., Legendre, B., Le Moel, A., and Yagoubi, N. (2001) Degradation of segmented poly(etherurethane) Tecoflex (R) induced by electron beam irradiation: characterization and evaluation. *Nucl. Instrum. Methods Phys. Res. B*, **185**, 100–107.
61 Zini, E. and Scandola, M. (2007) Shape memory behavior of novel (L-lactide-glycolide-trimethylene carbonate) terpolymers. *Biomacromolecules*, **8**, 3661–3667.
62 Zheng, X.T., Zhou, S.B., Li, X.H., and Weng, H. (2006) Shape memory properties of poly(D,L-lactide)/hydroxyapatite composites. *Biomaterials*, **27** (**24**), 4288–4295.
63 Zheng, X., Zhou, S., Yu, X., Li, X., Feng, B., Qu, S., and Wenig, J. (2008) Effect of *in vitro* degradation of poly(D,L-lactide)/β-tricalcium composite on its shape-memory properties. *J. Biomed. Mater. Res. B*, **86B** (**1**), 170–180.
64 Ferrera, D.A. (2001) Shape-Memory Polymer Intravascular Delivery System. US Patent, 6224610..
65 Yakacki, C.M., Shandas, R., Lanning, C., Rech, B., Eckstein, A., and Gall, K. (2007) Unconstrained recovery characterization of shape-memory polymer networks for cardiovascular applications. *Biomaterials*, **28** (**14**), 2255–2263.
66 Hampikian, J.M., Heaton, B.C., Tong, F.C., Zhang, Z.Q., and Wong, C.P. (2006) Mechanical and radiographic properties of a shape memory polymer composite for intracranial aneurysm coils. *Mater. Sci. Eng. C*, **26** (**8**), 1373–1379.
67 Frost and Sullivan (2008) N39F-54-20 Medical Device Technologies Changing Healthcare.
68 Lendlein, A., Behl, M., Hiebel, B., and Wischke, C. (2010) Shape-memory polymers as technology platform for biomedical applications. *Expert Rev. Med. Devices*, **7** (**3**), 357–379.
69 Sokolowski, W., Metcalfe, A., Hayashi, S., Yahia, L., and Raymond, J. (2007) Medical applications of shape memory polymers. *Biomed. Mater.*, **2** (**1**), S23–S27.
70 Maitland, D.J., Metzger, M.F., Schumann, D., Lee, A., and Wilson, T.S. (2002) Photothermal properties of shape memory polymer micro-actuators for treating stroke. *Laser Surg. Med.*, **30** (**1**), 1–11.
71 Wykrzykowska, J.J., Onuma, Y., and Serruys, P.W. (2009) Advances in stent drug delivery: the future is in bioabsorbable stents. *Expert Opin. Drug Deliv.*, **6** (**2**), 113–126.
72 Duarte, M.P., Maldjian, C.T., and Laskowski, I. (2009) Comparison of endovascular versus open repair of abdominal aortic aneurysms: a review. *Cardiol. Rev.*, **17** (**3**), 112–114.
73 Lederle, F.A. (2009) In the clinic. Abdominal aortic aneurysm. *Ann. Intern. Med.*, **150** (**9**), ITC5-1–ITC5-15.
74 Maitland, D.J., Small, W., Ortega, J.M., Buckley, P.R., Rodriguez, J., Hartman, J., and Wilson, T.S. (2007) Prototype laser-activated shape memory polymer foam device for embolic treatment of

aneurysms. *J. Biomed. Opt.*, **12** (**3**), 030504.

75 Gobin, Y.P., Starkman, S., Duckwiler, G.R., Grobelny, T., Kidwell, C.S., Jahan, R., Pile-Spellman, J., Segal, A., Vinuela, F., and Saver, J.L. (2004) MERCI 1: a phase 1 study of mechanical embolus removal in cerebral ischemia. *Stroke*, **35** (**12**), 2848–2854.

76 Metzger, M.F., Wilson, T.S., Schumann, D., Matthews, D.L., and Maitland, D.J. (2002) Mechanical properties of mechanical actuator for treating ischemic stroke. *Biomed. Microdevices*, **4** (**2**), 89–96.

77 Hayashi, S. (1993) Properties and applications of polyurethane-series shape-memory polymer. *Int. Prog. Urethanes*, **6**, 90–150.

78 Woodland, J.H. and Yolles, S. (1973) Long-acting delivery systems for narcotic antagonists. 1. *J. Med. Chem.*, **16** (**8**), 897–901.

79 Duvvuri, S., Janoria, K.G., and Mitra, A.K. (2006) Effect of polymer blending on the release of Ganciclovir from PLGA microspheres. *Pharm. Res.*, **23** (**1**), 215–223.

80 Liu, H., Finn, N., and Yates, M.Z. (2005) Encapsulation and sustained release of a model drug, Indomethacin, using CO_2-based microencapsulation. *Langmuir*, **21**, 379–385.

81 Wischke, C. and Schwendeman, S.P. (2008) Principles of encapsulating hydrophobic drugs in PLA/PLGA microparticles. *Int. J. Pharm.*, **364**, 298–327.

82 Göpferich, A. and Tessmar, J. (2002) Polyanhydride degradation and erosion. *Adv. Drug Deliv. Rev.*, **54**, 911–931.

83 Heller, J., Barr, J., Ng, S.Y., Schwach Abdellauoi, K., and Gurny, R. (2002) Poly(ortho esters): synthesis, characterization, properties and uses. *Adv. Drug Deliv. Rev.*, **54**, 1015–1039.

84 Neffe, A.T., Hanh, B.D., Steuer, S., and Lendlein, A. (2009) Polymer networks combining controlled drug release, biodegradation, and shape memory capability. *Adv. Mater.*, **21**, 3394–3398.

85 Wischke, C., Neffe, A.T., and Lendlein, A. (2010) Controlled drug release from biodegradable shape-memory polymers. *Adv. Polym. Sci.*, **226**, 177–205.

86 Wischke, C., Neffe, A.T., Steuer, S., and Lendlein, A. (2009) Evaluation of a degradable shape-memory polymer network as matrix for controlled drug release. *J. Control. Release*, **138**, 243–250.